

***N*-[6-(4-Butanoyl-5-methyl-1*H*-pyrazol-1-yl)pyridazin-3-yl]-5-chloro-1-[2-(4-methylpiperazin-1-yl)-2-oxoethyl]-1*H*-indole-3-carboxamide (SAR216471), a Novel Intravenous and Oral, Reversible, and Directly Acting P2Y₁₂ Antagonist**

Christophe Boldron,^{*,†} Angéline Besse,[†] Marie-Françoise Bordes,[†] Stéphanie Tissandié,[†] Xavier Yvon,[†] Benjamin Gau,[†] Alain Badorc,[†] Tristan Rousseaux,[†] Guillaume Barré,[†] Jérôme Menevrol,[†] Gernot Zech,^{||} Marc Nazare,[⊥] Valérie Fossey,[‡] Anne-Marie Pflieger,[†] Sandrine Bonnet-Lignon,[†] Laurence Millet,[†] Christophe Briot,[§] Frédérique Dol,[†] Jean-Pascal Héroult,[†] Pierre Savi,[†] Gilbert Lassalle,[†] Nathalie Delesque,[†] Jean-Marc Herbert,[†] and Françoise Bono[†]

[†]Sanofi R&D, 195 Route d'Espagne, 31036 Toulouse Cedex, France

[‡]Sanofi R&D, 1, Avenue Pierre Brossolette, 91385 Chilly-Mazarin Cedex, France

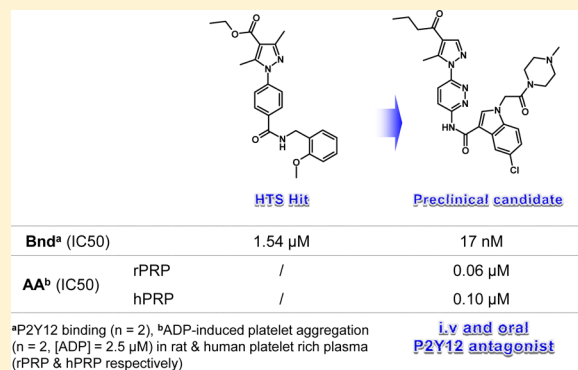
[§]Sanofi R&D, 371 Rue du Professeur Joseph Blayac, 34184 Montpellier, France

^{||}Sanofi R&D, Industriepark Hoechst, 65926 Frankfurt am Main, Germany

[⊥]AG Medizinische Chemie, Leibniz-Institut für Molekulare Pharmakologie, 13125 Berlin, Germany

S Supporting Information

ABSTRACT: In the search of a potential backup for clopidogrel, we have initiated a HTS campaign designed to identify novel reversible P2Y₁₂ antagonists. Starting from a hit with low micromolar binding activity, we report here the main steps of the optimization process leading to the identification of the preclinical candidate SAR216471. It is a potent, highly selective, and reversible P2Y₁₂ receptor antagonist and by far the most potent inhibitor of ADP-induced platelet aggregation among the P2Y₁₂ antagonists described in the literature. SAR216471 displays potent *in vivo* antiplatelet and antithrombotic activities and has the potential to differentiate from other antiplatelet agents.



■ INTRODUCTION

Platelets play a major role in the formation of arterial thrombosis originating from a lesion of the vascular wall or the rupture of an atherosclerotic plaque. Indeed they are activated by multiple factors such as the release of endogenous mediators from damaged endothelial cells, the exposure of thrombogenic molecules of the extracellular matrix of the damaged vessel, or high shear stress from stenosed vessels. After activation, platelets adhere and aggregate at the site of the vascular lesion, causing thrombi formation. Adenosine 5'-diphosphate (ADP) liberated from damaged red blood cells or endothelial cells is a key mediator of activation and aggregation of platelets. ADP could bind two purinergic receptors P2Y₁ and P2Y₁₂. P2Y₁ is implicated in platelet shape changes, whereas P2Y₁₂ is involved in platelet aggregation, thrombin generation, microparticles release, and thrombus stabilization.¹ Although binding of ADP to both receptors is required for complete platelet aggregation, P2Y₁₂ is the major receptor involved in

ADP-stimulated platelet activation of the glycoprotein (GP) IIb/IIIa.²

Historically, thienopyridines (ticlopidine and clopidogrel) were reported as the first orally active ADP antagonists (Figure 1). They were shown to display high levels of antithrombotic activity.^{3–5} Following the cloning of the P2Y₁₂ receptor,^{6,7} clopidogrel (FDA-approved in 1997) has been further demonstrated to bind irreversibly to the receptors through a thiol active metabolite following two oxidative biotransformations. The therapeutic success of these P2Y₁₂ receptor inhibitors in preventing atherothrombotic events in patients after an experience of acute coronary syndrome (ACS), especially those undergoing percutaneous coronary intervention (PCI), has definitely provided evidence that P2Y₁₂ antagonism is a key therapeutic target in the management and prevention of arterial thrombosis.⁸ Prasugrel (Figure 1),⁹

Received: April 15, 2014

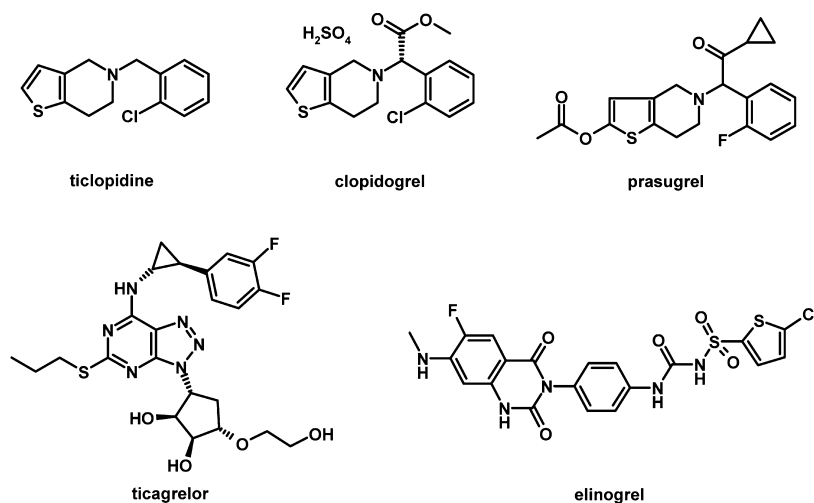


Figure 1. Reference P2Y12 antagonists.

approved in 2009, is a prodrug analogue of the first biotransformed intermediate of clopidogrel, therefore requiring only one oxidative step to generate a thiol active metabolite.^{10,11} Similar to clopidogrel, prasugrel activity is exerted through an irreversible binding to the P2Y12 receptor. Ticagrelor, approved in 2011 for coronary artery disease (CAD) and ACS, is the result of an impressive program of medicinal chemistry aiming at transforming ATP, the natural antagonist of ADP receptors, into an orally active, reversible antagonist of P2Y12 (Figure 1).¹² More recently, elinogrel (Figure 1), originating from a HTS hit and further optimization, was developed as both iv and po antithrombotic agent until phase II studies, but its clinical development was unfortunately stopped in 2012.¹³ Although clopidogrel is still a treatment of choice for most of arterial diseases, we were wondering whether an iv/po reversible antagonist displaying a fast onset of action with less susceptibility for interindividual variability and less bleeding risk would complement clopidogrel treatments.

Starting from a HTS hit with micromolar binding activity, we report here how we improved in vitro and in vivo antiplatelet activities together with several key ADME parameters, thus leading to the identification of a preclinical candidate.

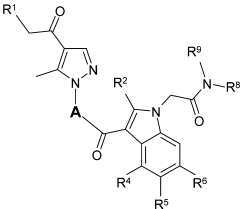
RESULTS AND DISCUSSION

Medicinal Chemistry Optimization. (Compound code numbers are depicted in Table 1.) A high throughput screening (HTS) campaign of the Sanofi compound collection was set using as primary assay the measurement of the down regulation of cAMP in the presence of Forskoline on CHO-CRE-Luc stimulated by 2-methylthio-ADP. Hits were confirmed using a binding assay involving two partners: radiolabeled thiomethyl-ADP and P2Y12-transfected CHO cells (will be referred as to Bnd assay in the text). Among the most potent hits, a 4-pyrazol-1-ylbenzamide chemical series was identified (Figure 2). The best representative member of the family was compound A₁ (HTS hit) that displayed micromolar IC₅₀ in the binding assay. By use of this scaffold, novel substructure and similarity searches were undertaken within the corporate database as well as commercially available collections in order to perform a backscreening aiming to test close analogues of HTS hits that were not included in the HTS core list. A backscreening hit bearing a urea in place of the amide linker

(compound A₂) showed a slight improvement in the ADP-induced platelet aggregation assay on washed platelets (IC₅₀ = 4.5 μM). An additional optimization run was then initiated (about 350 new molecules synthesized). Compound A₃, bearing a butanoic side chain connected through an alkoxy group at the ortho position of the urea linker, revealed some key structural features that allowed marked activity improvements in the Bnd assay (Figure 2, IC₅₀ = 80 nM). Then further improvements were made possible by inserting a methyl group in the para position of the anisole group. In the last part of the optimization run, the metabolically labile pyrazole-4-carboxylic ethyl ester was replaced by a pyrazole-4-butan-1-one motif, thus leading to the identification of compound A₄, a potent and metabolically stable P2Y12 antagonist (Bnd, IC₅₀ = 17 nM), which was nominated as “intermediate lead”. However, significant potency loss was observed with intermediate lead A₄ in the ADP-induced platelet aggregation assays (will be referred as to AA in the text) in rat and human platelet rich plasma (will be referred as to rPRP and hPRP, respectively).

Always bearing in mind our goal to identify orally bioavailable P2Y12 antagonists, we have attempted simple modifications such as monomethylation of both urea nitrogen atoms, replacement of the urea by up and down amide, acetamide, 2-oxo-acetamide, or 2-aminoimidazole linkers without success (Figure 2). An important SAR element was the loss of activity while replacing the oxygen atom from anisole by a methylene group, thus making this *o*-aminoanisole group mandatory for reaching a high level of activity (compounds A₃ and A₄). We made the hypothesis that the molecule could be locked in an active conformation because of a H-bonded five-membered ring between the urea NH and the oxygen atom in the ortho position (Figure 3). Such a H-bond stabilization was already demonstrated by Etter et al. after X-ray diffraction of monocrystals of *o*-alkoxybiphenylurea derivatives.¹⁴ To experiment with this hypothesis, we simply replaced the *o*-aminoanisole by an indole connected to the carbonyl group via the 1-position (48) or via the 3-position (47). We were delighted to see that these modifications did not affect the biological activities (Figure 3). As 48 was shown to be sensitive to degradation in mild basic and acidic conditions, we decided to focus our next efforts around compound 47. Importantly, this successful rescaffolding reduced the number of H-bond donors and acceptors, making this new platform a good starting

Table 1. Compound Code Numbers



	A	R ¹	R ²	R ⁴	R ⁵	R ⁶	Final compounds	
a		Et			Me		52a, 53 to 97	
b		Et			Me		-	
c		Et			Me	Me	51, 52c	
d		Et		Me	Me		-	
e		Et	Me		Me		-	
f		Et			Br		-	
g		Et			OMe		52g	
h		Et			Cl		52h, 98 to 104	
i		Me			Cl		52i	
j		H			Cl		52j	
k			CF ₃ CH ₂			Cl		52k
l			Et			Cl	F	52l
m			Et			Br	Me	52m
n			Et			CF ₃		52n
o			Et			Cl	Me	52o
p		Et			CN		52p	
q		Et			Me	Br	52q	
r		Et			Me	Cl	52r	
s		Et			Cl	Cl	52s	
t		Et			F		52t	
u		Et				Me	52u	
p'		Et			C(O)NH ₂		52p'	
v		Et			Cl		-	
w		Et			Cl		52w	
y		Et			Cl		52y	
z		Et			Cl		52z	
aa		Et			Cl		52aa	
ab		Et			Cl		52ab	
ac		Et			Cl		52ac	
ad		Et			Cl		52ad	
ae		Et			Cl		52ae	
af		Et			Cl		52af	
ak		Et			Cl		52ak	

point on the path to orally bioavailable compounds. The next stage of the optimization process was to improve the functional activity. Interestingly, decreasing the length of the COOH-bearing side chain of 47 by one methylene (49) or two methylene groups (50a) dramatically improved biological activities (Figure 4). However, a significant discrepancy should be noted when comparing functional activities in humans and rats. A "methyl scan" of 50a (IC₅₀ values: Bnd 0.9 nM; AA (hPRP) 1.8 μM; AA (rPRP) 9.7 μM) was performed in order to better apprehend the active conformation and/or the key points of interaction with the P2Y₁₂ receptor (Table 2). Methylation at the amide linker or at C-2 and C-4 positions of the indole motif (compounds 50b, 50e, and 50d, respectively)

appeared to be deleterious for biological activities. Interestingly, methyl insertion at C-6 positions (compound 50c), while decreasing binding activity, was very much favorable regarding the functional activity in both species. Surprisingly, the quite acceptable and nonspecies dependent functional activity of 46a, ester analogue of 50a, was unexpected given its modest IC₅₀ of binding. This result confirmed the role played by the carboxylic acid group in term of both functional potency and species discrepancy. When we were working on COOH-containing urea derivatives, we had observed a significant decrease of the binding activities by a factor of 5–50 when performing binding experiments in the presence of 80 g/L human serum albumin (HSA, mean normal blood concentration of ~50 g/L),¹⁵ thus revealing a strong capacity to bind plasma proteins. In this regard and when compounds 50a and 46a are compared, methyl ester removes and inhibits the interaction of free carboxylic acid to serum albumin. In order to avoid bias related to binding experiments conditions, we decided to make the lead selection based on the *in vitro* functional activity (AA).

Thus, 50c was considered as the new lead compound, as it allowed reaching for the first time submicromolar activities in the *in vitro* AA assay on hPRP. Because of the carboxylic acid group, compounds 50a and 50c were found to be metabolically stable in rat and human microsomal fractions but, by contrast, not permeable on Caco2 cells (Table 3). As shown with compound 46a, the carboxy group seemed not to be absolutely mandatory for the functional activity. As we did not want to move further through the optimization of an ester prodrug, we exploited this finding by undertaking the preparation of amide derivatives. Behaving in the same manner as 46a, compound 51 (dimethylcarboxamide analogue of 50c) exhibited submicromolar functional activity in hPRP despite a significant loss of activity in the binding assay when compared to 50c (Table 3). Interestingly, primary carboxamide and monomethylcarboxamide analogues displayed similar activities as 51 (Bnd, 31 and 47 nM respectively; AA on hPRP, 2.0 and 1.0 μM, respectively). These results clearly confirmed carboxamide derivatives as good candidates for carboxylic acid replacement. In addition to retaining the functional activity, 51 also showed a high level of permeation on Caco2 cells which was promising as part of our aim to identify orally bioavailable compounds. Unfortunately, 51 was found to be metabolically unstable on microsomal fractions. In order to address the low solubility of 51, we then prepared the methylpiperazine analogue 52c. Very interestingly, 52c appeared to be biologically more active than 51, quite permeable, but still sensitive to oxidative metabolism. Suspecting benzylic positions to represent metabolic hot spots, we removed one methyl group to generate a potent P2Y₁₂ antagonist (compound 52a) displaying more acceptable levels of oxidative metabolism in rat and human species and, because of the piperazinyl motif, a large increase of aqueous solubility up to 0.76 mg/mL (Table 3). 52a displayed a medium *in vitro* permeability on Caco2 cells and was appointed as pharmacological tool for a preliminary *in vivo* evaluation. In the meantime and building on these promising results achieved with the methylpiperazine motif, we have prepared a series of carboxamide derivatives also bearing a basic nitrogen atom whose role was to ensure an acceptable solubility. The representative and nonexhaustive list of compounds synthesized is given at Table 4 and could be divided in three subgroups: subgroup 1, compounds 53–63 ⇒ carboxamides connected through a noncyclic amino group; subgroup 2, compounds 64–77 ⇒ nonpiperazinyl-containing carboxamides

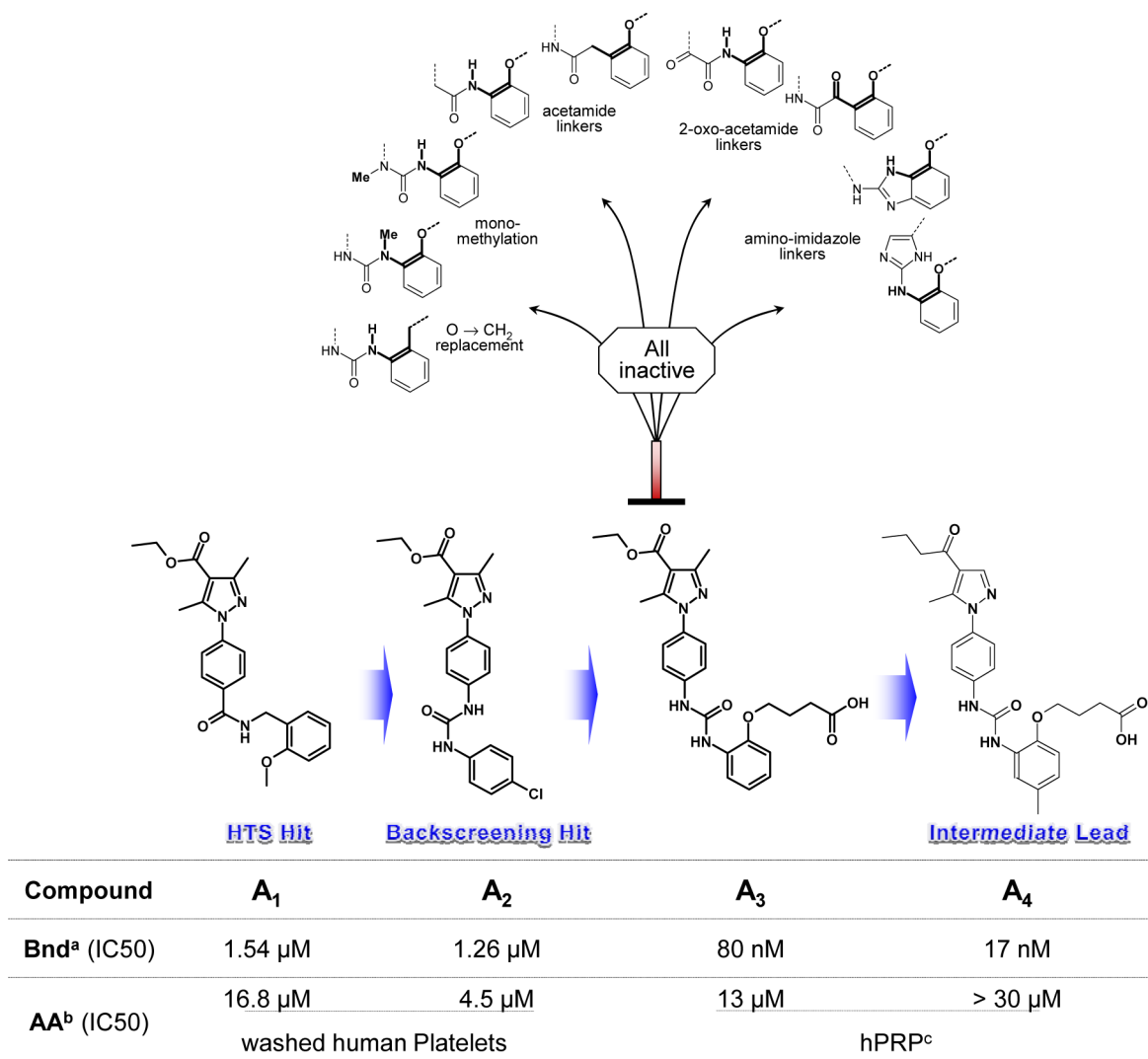


Figure 2. HTS phenylpyrazole hit series. Footnotes for the table are the following: ^aP2Y₁₂ binding ($n = 2$); ^bADP-induced platelet aggregation ([ADP] = 2.5 μM, $n = 2$), chuman platelet rich plasma (hPRP).

connected through a cyclic amino group; subgroup 3, compounds **52a** and **78–97** ⇒ piperazinylcarboxamide-containing derivatives. All these compounds have been biologically evaluated using “Bnd” and “AA in rPRP” assays. Indeed, as mentioned before with compound **46a**, carboxamide derivatives did not display species discrepancies anymore (see Table 3). Therefore, evaluation on rat samples (instead of humans) was preferred for obvious reasons of plasma accessibility. The selection of potential in vivo pharmacological tools was done using an empirical value that we called the eligibility factor (EF). EF was the result of the multiplication of “Bnd” in nM by “AA in rPRP” in μM and reflected the balance between functional and binding activities. We posed the rule that compounds to be selected for in vivo evaluation should display EF values below 20. This simple equation was born from the observation that displaying submicromolar functional activities was not a sufficient condition for a compound to be active in vivo. Indeed, it had to be associated with a good enough activity of binding. This rule has been tested and challenged with success right from the start of the advanced program phase. One typical example for illustration is compound **85** which was found to be inactive ex vivo (15% ± 2) after a 10 mg/kg oral administration. This compound

displayed a high level of functional activity (IC₅₀ = 0.4 μM), an ADME profile very similar to those of ex vivo active compounds displayed in Figure 5 but a relatively low activity of binding (IC₅₀ = 82 nM).

Among the 46 compounds displayed in Table 4, it appeared very clearly that piperazinyl-containing derivatives were very much preferred, as no member from subgroups 1 and 2 were elected. Ethylenediamine-, aminopyrrolidine-, and aminopiperidine-containing derivatives all displayed high IC₅₀ values of binding that were not compensated by good enough AA in rPRP, thus generating high EF. In addition, there seem not to be any hydrogen bonding to the receptor in this region, as shown by the similar levels of activity between non-, mono- and dimethylated amines. Only compound **77** was found to be borderline with an EF of 23. It was very interesting to note that within subgroups 1 and 2, the 2-methyloctahydropyrrolo[3,4-*c*]pyrrole motif from **77** was by far the most analogous to the methylpiperazine motif from **52a** in terms of “3D shape”. This reinforced our desire to go further with piperazinyl-containing derivatives. Removing the methyl from the methylpiperazine motif (**90**), increasing the length from methyl to ethyl and *n*-butyl (**52a**, **78**, **79**), or inserting ramified or cyclic alkyl groups (**82**, **83**, **84**, and **85**) was not beneficial. The insertion of an

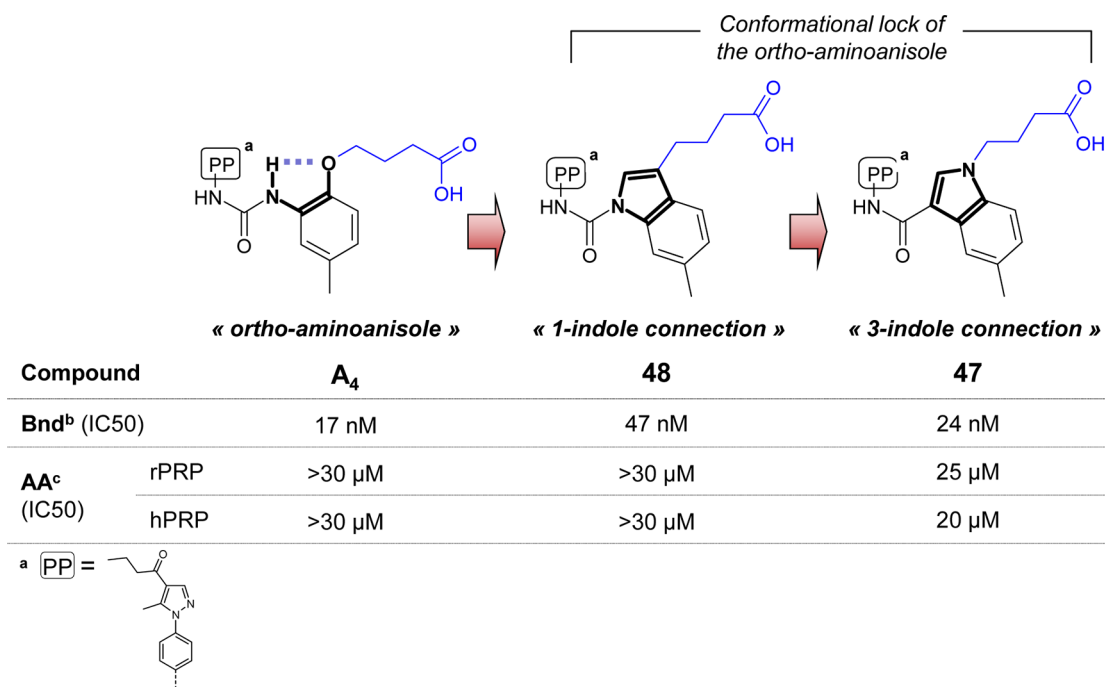


Figure 3. *o*-Aminoanisoole resc scaffolding. Footnotes for the table are the following: ^achemical structure as shown below table; ^bP2Y₁₂ binding ($n = 2$); ^cADP-induced platelet aggregation ([ADP] = 2.5 μM, $n = 2$) in rat and human platelet rich plasma (rPRP and hPRP, respectively).

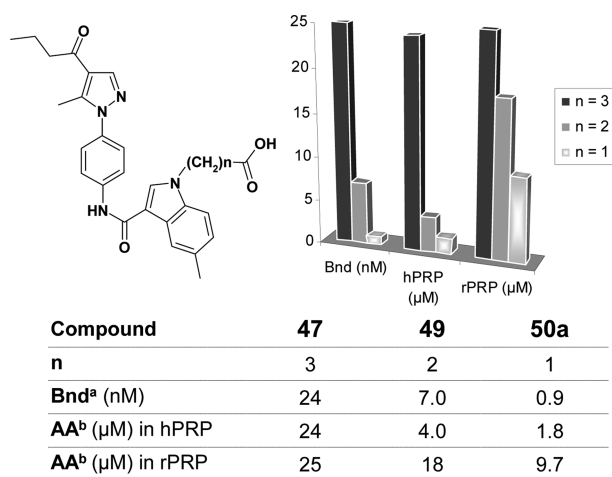


Figure 4. Modification of the COOH-bearing side chain. Footnotes for the table are the following: ^aP2Y₁₂ binding ($n = 2$); ^bADP-induced platelet aggregation ([ADP] = 2.5 μM, $n = 2$) in rat and human platelet rich plasma (rPRP and hPRP, respectively).

ethyl side chain bearing one or two heteroatoms (**80**, **81**, **91**, and **92**) led to very potent compounds displaying EFs down to 6. The trifluoroethyl analogue **93** was found to be much less active. From the set of compounds bearing one or two methyl groups at the α position of the basic nitrogen (**86**, **87**, **88**, **89**) or a methylene group bridging the 2- and 5-piperazinyl positions (**95** and **96**), only compound **87** was elected. Very potent compounds were also identified bearing either a 3-methyloctahydropyrrolo[1,2-*a*]pyrazin-7-ol motif (**94**) or a *p*-fluorobenzyl group (**97**).

At this point in the optimization and regarding the high level of in vitro functional activity reached, we moved to an in vivo proof of concept (POC). Seven new compounds, in addition to **52a**, met the EF rule (shaded lines in Table 4). We first checked their liability on rat microsomal fractions, and as they

Table 2. “Methyl Scan” around Compound **50a**

compd	R ¹	R ²	R ⁴	R ⁶	Z	Bnd ^a (nM)	AA ^b (μM) in hPRP	AA ^b (μM) in rPRP
50a	H	H	H	H	OH	0.9	1.8	9.7
50b	Me	H	H	H	OH	304	>30	>30
50e	H	Me	H	H	OH	84	15	16
50d	H	H	Me	H	OH	272	>30	>30
50c	H	H	H	Me	OH	5.1	0.4	4.6
46a	H	H	H	H	OMe	93	4.1	3.5

^aP2Y₁₂ binding ($n = 2$). ^bADP-induced platelet aggregation ($n = 2$, [ADP] = 2.5 μM) in rat and human platelet rich plasma (rPRP and hPRP, respectively).

all displayed low to medium level of oxidative metabolism, we decided to evaluate them in our standard ex vivo inhibition of platelet aggregation model after an oral dosing of 10 mg/kg in rats (Figure 5). Three out of 8 tested compounds (**81**, **91**, and **97**) exhibited high levels of ex vivo inhibition in good correlation with their low EF values. **52a** and **87** were found to be borderline in term of oxidative metabolic stability on rat microsomal fractions which may justify their lower ex vivo activity in rats. Surprisingly, **92** was found to be much less active in vivo than **91** despite that it was as active in vitro and it displayed similar metabolic and permeability parameters. This

Table 3. SAR Optimization: From Carboxylic Acid to Carboxamide Derivatives

Compound	50a	50c	51	52c	52a	
R =						
		SAR enrichment (functional activity ↑)	Carboxylic acid replacement (permeation issue)	Insertion of a basic moiety (solubility issue)	Removal of one benzylic position (metabolic issues)	
Bnd ^a (nM)	0,95	5,1	31	39	31	
AA ^b (IC ₅₀) in μM	hPRP rPRP	1,8 9.7	0.4 4.6	0.8 2.2	0.5 0.5	
Permeability Caco-2 ^c	0	0	186	59	40	
% Metabolism ^d	Hum rat	5 1	4 2	59 64	50 52	39 41
Water solubility in mg/mL (final pH)	ND	ND	< 0.01	ND	0.76 (4.9)	

OK Borderline Issue

^aP2Y₁₂ binding ($n = 2$). ^bADP-induced platelet aggregation ($n = 2$, [ADP] = 2.5 μM) in rat and human platelet rich plasma (rPRP and hPRP, respectively). ^cPermeability measured on a Caco2 cells monolayer (expressed in 10⁻⁷ cm·s⁻¹). ^dIncubation with hepatic microsomal fractions during 20 min in the presence of 1 mM NADPH (e.g., 5% metabolism means for 95% of unchanged compound).

Table 4. First Part of the Carboxamide Optimization (5-Methylindole Platform)

Cpd	NR ² R ³	Bnd ^a (nM)	AA ^b (μM) in rPRP	EF ^c	Cpd	NR ² R ³	Bnd ^a (nM)	AA ^b (μM) in rPRP	EF ^c	Cpd	NR ² R ³	Bnd ^a (nM)	AA ^b (μM) in rPRP	EF ^c	Cpd	NR ² R ³	Bnd ^a (nM)	AA ^b (μM) in rPRP	EF ^c
		61	1.7	104	58		61	1.7	104	52a		31	0.5	16	88		102	0.4	41
59		88	1.8	158	69		46	1.1	51	78		66	0.9	59	89		28	0.8	22
60		139	1.0	139	70		65	1.0	65	79		121	0.9	109	90		26	1.0	36
61		47	0.8	38	71		73	1.1	80	80		41	0.4	16	91		19	0.4	8
62		71	1.0	71	72		111	0.5	56	81		20	0.3	6	92		19	0.5	10
63		84	0.9	76	73		100	1.4	140	82		29	1.7	49	93		66	1.1	73
Subgroup 1					Subgroup 2					Subgroup 3									
53		61	0.8	49	74		117	1.0	117	83		44	0.8	35	94		15	0.5	8
54		94	1.5	141	75		89	1.4	125	84		76	0.7	53	95		86	0.5	43
55		92	1.0	92	76		106	0.4	42	85		82	0.4	33	96		70	1.2	84
56		194	4.0	776	77		33	0.7	23	86		46	0.7	32	97		12	0.4	5
57		124	1.0	124	67		94	1.1	103	87		27	0.4	11					

^aP2Y₁₂ binding ($n = 2$). ^bADP-induced platelet aggregation ($n = 2$, [ADP] = 2.5 μM) in rat platelet rich plasma (rPRP). ^cEligibility factor = Bnd (nM) × AA in rPRP (μM). Shaded cells correspond to compounds selected for in vivo evaluation, as they display EF values of <20.

might be the result of a decrease in solubility consequent to the presence of the second fluorine atom that decreased the piperidine pK_a. However, we could not exclude the possibility that **91** ex vivo activity was further enhanced because of an irreversible binding to the receptor either through a direct substitution of the aliphatic C–F bond or via the intermediary formation of an electrophilic aziridinium (short duration of in vitro assays would limit the formation of such a covalent adduct). Considering this hypothesis, **92** was much less amenable to such an irreversible binding. In doubt, we excluded this fluoroethyl motif from any further investigations following the initial specifications to identify a reversible P2Y₁₂ antagonist. As suggested by their low Caco2 permeation values, the capacity of compounds **80** and **94** to cross the

gastrointestinal barrier was probably hampered by the presence of the hydroxyl group (Figure 5).

Unfortunately, **81** and **97** displayed a high level of oxidative metabolism in human microsomal fractions, not making them suitable for further investigations. However, this encouraging ex vivo POC with **81**, **91**, and **97** comforted us in regard to the translatability of in vitro results into ex vivo activities after oral administration. We then focused our efforts through the identification of oxidatively more stable compounds. Since the most obvious metabolic hot spot shared by these last compounds was the benzylic position, we undertook the optimization of the indole substitution pattern. We decided to proceed using a 4-methylpiperazinylcarboxamide platform, since this motif appeared to provide the best balance between

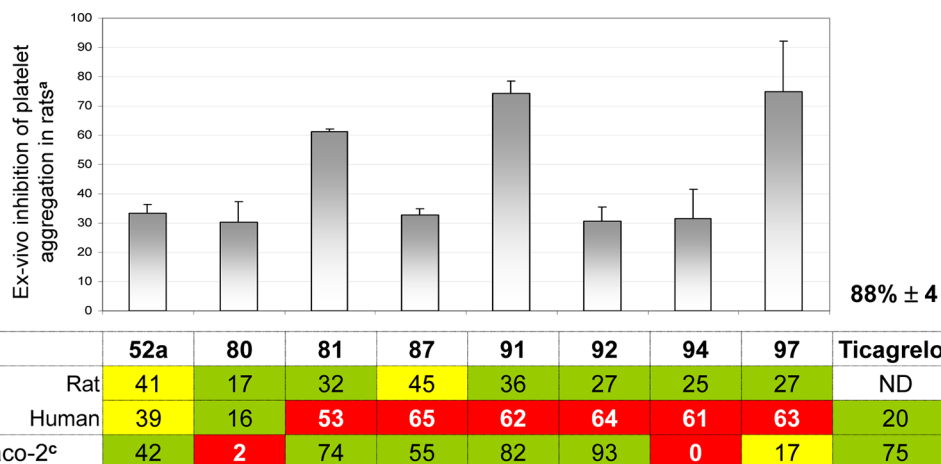
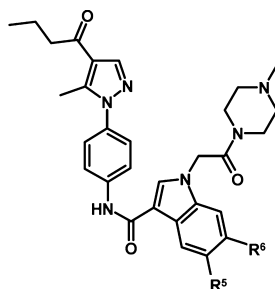


Figure 5. Ex vivo inhibition of platelet aggregation in rats 2 h after a 10 mg/kg oral dosing. Footnotes for the table are the following: ^aadministration of a 10mg/kg oral dose; ^bincubation with hepatic microsomal fractions during 20 min in the presence of 1 mM NADPH (e.g., 41% metabolism means for 59% of unchanged compound); ^cpermeability measured on Caco2 cells monolayer (expressed in 10^{-7} $\text{cm}\cdot\text{s}^{-1}$).

Table 5. Indole Optimization



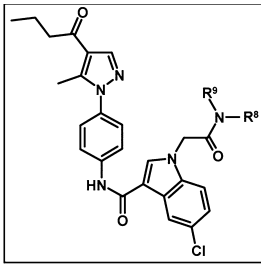
compd	R ⁵	R ⁶	Bnd ^a (nM)	AA ^b (μM) in human PRP	AA ^b (μM) in rat PRP	EF ^c	% metabolism on microsomal fractions ^e		Caco2 permeation ^d	ex vivo inhibition ^f
							human	rat		
52c	Me	Me	39	0.5	0.3	12	50	52	59	37 \pm 5
52a	Me	H	31	0.5	0.5	16	39	41	40	33 \pm 3
52g	OMe	H	22	0.4	0.5	11	68	63	0	ND
52h	Cl	H	27	0.5	0.4	11	36	14	16	50 \pm 5
52l	Cl	F	48	0.5	0.3	14	31	21	11	inactive
52m	Br	Me	48	1.1	0.4	19	34	20	28	21 \pm 4
52n	CF ₃	H	50	0.7	0.4	20	15	14	9	26 \pm 8
52o	Cl	Me	34	0.5	0.6	20	36	23	36	31 \pm 2
52p	CN	H	76		2.3	175				
52q	Me	Br	118		1.7	200				
52r	Me	Cl	138		2.0	276				
52s	Cl	Cl	99		3.7	366				
52t	F	H	142		2.7	383				
52u	H	Me			5.4					
52p'	(CO)NH ₂	H			5.9					

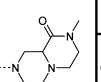
^aP2Y₁₂ binding ($n = 2$). ^bADP-induced platelet aggregation ($n = 2$, [ADP] = 2.5 μM) in human or rat platelet rich plasma (hPRP or rPRP, respectively). ^cEligibility factor = Bnd (nM) \times AA in rPRP (μM). ^dPermeability measured on a Caco2 cells monolayer (expressed in 10^{-7} $\text{cm}\cdot\text{s}^{-1}$). ^eIncubation with hepatic microsomal fractions during 20 min in the presence of 1 mM NADPH (e.g., 52% metabolism means for 48% of unchanged compound). ^fEx vivo inhibition of platelet aggregation in rats (%), 2 h after a 10 mg/kg oral dosing.

oxidative metabolism and Caco2 permeation. The nonexhaustive list of modified indole-containing derivatives is given in Table 4. We followed the same decision tree as before (AA in rPRP, yes/no \rightarrow Bnd, yes/no \rightarrow AA in hPRP, yes/no \rightarrow ex vivo when $\text{EF} \leq 20$). Substituents such as a fluorine atom

(52t), a nitrile (52p), or a primary carboxamide (52p') at position 5 were not tolerated. Moving the methyl group from position 5 in 52a to position 6 in 52u was detrimental, which was somehow unexpected because the 5,6-dimethylindole derivative 52c was found to be active. The combination of a

Table 6. Second Part of the Carboxamide Optimization (5-Chloroindole Platform)



Cpd	NR ⁹ R ⁹	Bnd ^a (nM)	AA ^b (μM) in human PRP	AA ^b (μM) in rat PRP	EF ^c	% metabolism on microsomal fractions ^e		Caco2 permeation ^d 10 ⁻⁷ cm/s	Ex-vivo inhibition of platelet aggregation in rats (%; 10 mg/kg)		
						human	Rat		2h	6h	
52h		27	0.5	0.4	11	36	14	16	50 ± 5	51 ± 7	
98		15	0.3	0.4	6	47	11	43	68 ± 0	65 ± 2	
99		11	0.3	0.2	2	14	6	0	22 ± 5	ND	
100		11	0.4	0.3	3	28	7	0	Inactive	ND	
101		11	0.3	0.2	2	87	31	6	72 ± 5	60 ± 8	
102		racemic	8	0.2	0.3	2	50	40	36	80 ± 10	39 ± 14
103		D-enantiomer	7	0.3	0.3	2	52	23	32	46 ± 5	Inactive
104		L-enantiomer	12	0.5	0.4	5	47	7	28	80 ± 4	61 ± 6

^aP2Y₁₂ binding ($n = 2$). ^bADP-induced platelet aggregation ($n = 2$, [ADP] = 2.5 μM) in human or rat platelet rich plasma (hPRP or rPRP, respectively). ^cEligibility factor = Bnd (nM) × AA in rPRP (μM). ^dPermeability measured on a Caco2 cells monolayer (expressed in 10⁻⁷ cm·s⁻¹). ^eIncubation with hepatic microsomal fractions during 20 min in the presence of 1 mM NADPH (e.g., 36% metabolism means for 64% of unchanged compound).

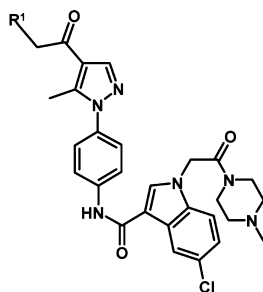
methyl group at position 5 with a halogen atom at position 6 (52q and 52r) or the combination of two chlorine atoms (52s) produced less active compounds. Interestingly, the methyl/halogen combination the other way around (52m and 52o) was much tolerated. Although it was found to be potent in vitro, the 5-OMe derivative 52g was not evaluated in vivo, as it displayed both a high level of metabolic transformation on rat microsomal fractions and a low Caco2 permeation. Five out of six new in vitro active compounds displaying EF below 20 (52h, 5-Cl; 52l, 5-Cl, 6-F; 52m, 5-Br, 6-Me; 52n, 5-CF₃; 52o, 5-Cl,6-Me) were found to be metabolically more stable than 52a, especially on rat microsomal fractions. We also observed a slight loss of permeation capability on Caco2 cells. Although we met our goal to identify in vitro active compounds less susceptible to oxidative metabolism, stability on human microsomal fractions was acceptable but not markedly reduced. We then evaluated them in the ex vivo inhibition of platelet aggregation model (2 h, 10 mg/kg oral, Table 5). Very interestingly, the 5-chloroindole derivative 52h was found to be significantly more active than compound 52a in the same conditions and was shown to respond in a dose dependent manner with an ED₅₀ of 11.1 mg/kg (data not shown). The other five compounds did not show any improvement and remained stuck below 30% inhibition of ex vivo platelet aggregation. Very interestingly, 52h was also found to be active in this ex vivo model after iv administration (30 min, I% (1 mg/kg) = 53 ± 18, I% (3 mg/kg) = 70 ± 8, and I% (10 mg/kg) = 86 ± 5). Before moving forward, we were willing to know more about the metabolic behavior of 52h in the human context and we were very pleased to see a major improvement from a high in vitro hepatic clearance on human hepatocytes with 52a

(0.150 mL/h) to a moderate one with 52h (0.100 mL/h). The metabolic hot spots were revealed after incubation on human microsomal fractions and human hepatocytes. Three main metabolites were produced in equal proportions (UV-LCMS detection) and were the result of (i) indole monohydroxylation, (ii) piperazine demethylation, and (iii) *n*-propyl side chain oxidation. Despite 52h displaying a potent and long-lasting ex vivo activity together with an acceptable projection in term of liver metabolism in the human context, we decided to operate some chemical modifications aiming to reduce further the metabolic liability. The optimization of the indole part of the molecule was discussed above (Table 5), and we already concluded that 5-chloroindole was the best motif. We then focused on the methylpiperazinyl motif, and leveraging our previous experience around compound 52a, we prepared more than 100 piperazine-containing carboxamide derivatives. Compounds 98–104 were found to be very much active in vitro (EF values down to 2) and were selected as representative examples, as they illustrate the difficulty we faced to adjust the permeation to metabolism balance within this chemical series (Table 6). Compound 98, bearing a methoxyethyl side chain, displayed a high level of Caco2 permeation together with a good metabolic stability on rat microsomal fractions leading to a strong (60–70% platelet aggregation inhibition) and long-lasting ex vivo activity (plateau up to 6 h after administration). Unfortunately, this compound appeared to be much too metabolized on human microsomal fractions (47% of liability) and human hepatocytes (hepatic clearance of 0.124 mL/h) for being further investigated. 101 and 102 were found to be particularly potent after oral administration (72% and 80% inhibition, respectively, 2 h after administration) but were not

selected for the same reasons as **98**. As expected, the oxidative metabolism was largely reduced while moving from methoxy to hydroxy group (compound **99** = main metabolite formed after incubation of **98** on microsomal fractions). However, as a consequence of the polarity increase, we observed the concomitant loss of Caco2 permeation and oral ex vivo activity. Similar to **99**, compound **100** bearing an acetamide fragment was found to be inactive ex vivo. The two isolated enantiomers from **102** displayed very similar in vitro biological activities, Caco2 permeation, and metabolic stability. Indeed, both were found to be very potent in vitro, confirming that the stereochemistry in this region of the molecule did not affect the interaction with the receptor. Very interestingly, the D-enantiomer **103** was found to be much less potent in vivo than its L-counterpart **104**, revealing an impact of the stereochemistry on the compound bioavailability that was apparently not related to permeation and oxidative metabolism. As a conclusion and similar to the work done around **52a**, we had to admit that the efforts to replace the methylpiperazine motif had been vain.

We already knew from previous studies in the original biphenylurea series but also during some works around compound **50a** that the biological activity was very sensitive to the replacement of the 1-(5-methyl-1H-pyrazol-4-yl)butan-1-one motif. As a result, we were not prone to make dramatic modifications and we finally focused on simple ones among which the most representative are depicted at Table 7.

Table 7. Optimization of Pyrazole Substitution



compd	R ¹	Bnd ^a (nM)	AA ^b (μM) in rat PRP	EF ^c	% metabolism on microsomal fractions ^d	
					human	rat
52h	CH ₂ CH ₃	27	0.4	11	36	14
52i	CH ₃	336	0.6	201	32	25
52j	H	143	0.7	100	40	47
52k	CH ₂ CF ₃	574	8	4592	6	3

^aP2Y₁₂ binding ($n = 2$). ^bADP-induced platelet aggregation ($n = 2$, [ADP] = 2.5 μM) in rat platelet rich plasma (rPRP). ^cEligibility factor = Bnd (nM) × AA in rPRP (μM). ^dIncubation with hepatic microsomal fractions during 20 min in the presence of 1 mM NADPH (e.g., 36% metabolism means for 64% of unchanged compound).

Shortening of the alkyl side chain (**52i** and **52j**) appeared detrimental for the biological activity and did not protect from oxidative metabolism. Very interestingly, the insertion of three fluorine atoms at the extremity of the *n*-propyl side chain (**52k**) produced a compound much less sensitive to oxidative metabolism. Unfortunately, this modification was not applicable, as **52k** appeared to be inactive.

At this stage of the optimization, it appeared clearly that **52h** was the best compromise between in vivo potency/duration of action in rats and predicted metabolism in humans. Although several compounds have shown higher levels of ex vivo antiaggregant activity in rats (compounds **81**, **91**, **97**, **98**, **101**, and **104**), we systematically had to face an extensive metabolic liability on human liver components.

Projecting farther to the required conditions necessary before considering a development candidate, we came to debate about the presence of an aniline motif that could be released upon cleavage of the central carboxamide linker of **52h** in biological media. This aniline fragment was found to be positive in the Ames assay after metabolic activation.¹⁶ It is very important to note that **52h** was found to be negative in the same assay with or without metabolic activation. Many ethical, biological, and technical challenges did not encourage us to try to demonstrate whether this aniline fragment and its mutagenic metabolite(s) were generated or not in vivo. Indeed, there is no threshold value for mutagenicity, which means that a single molecule could be responsible for it. The diversity and the chemical reactivity of the expected metabolites make it even more complex. In view of that, it appeared inconceivable to reach conclusions that would be strong enough to convince ourselves and competent authorities about the long-term safety of compound **52h**. Therefore, we decided to initiate a second MedChem optimization phase aiming to get rid of this aniline fragment.

As generally observed, the aniline fragment was not found to be mutagenic in the absence of metabolic activation. Because bacteria are unable to metabolize chemicals like CYP does, a key component for making the Ames test useful in that particular case is the inclusion of S9 microsomal fractions as an exogenous mammalian metabolic activation system.¹⁷ Indeed, to exert their mutagenic potential, aromatic amines or their acetylated analogues (from aniline acetylation by acetyl CoA) have to be transformed into reactive electrophiles (Scheme 1). The first metabolic step leading to these reactive species is a CYP-mediated N-oxidation that produces hydroxylamine intermediates that can undergo N–O bond cleavage to form arylnitrenium ions. Alternatively, further bioactivation of the *N*-hydroxylamine derivatives to *N*-acetoxy or *N*-sulfate esters makes the N–O bond heterolysis easier and/or the DNA-adducts formation through a S_N2 reaction with DNA possible.¹⁸ Then the nitrenium ion is trapped by DNA, where it binds covalently through nitrogen N atom directly or through the C atom at the ortho position, essentially at guanine nucleic bases (Scheme 1).¹⁹ These genetic alterations might then result in mutagenesis and carcinogenesis.

Several QSAR equations displaying accuracies of about 80–90% have been drawn from the large aniline mutagenicity and carcinogenicity databank. The identification of some key molecular determinants came from these intensive investigations.²⁰ The probability of inducing mutagenicity was found to be closely related to physicochemical factors that modulate the oxidation capacity of the amino group which is the first step on the course to the generation of the arylnitrenium (Scheme 1). The most relevant factors appeared to be the hydrophobicity, the energy of the highest occupied orbital (HOMO) and of the lowest unoccupied orbital (LUMO), and the steric hindrance ortho to the amino group. Hydrophobicity is involved in the absorption and the transport of the drugs in cells (hepatocytes for instance) and organisms, as well as in the interaction between drugs and the metabolizing enzymes. The electronic

Scheme 1. General Mechanisms Leading to Aniline Mutagenesis/Carcinogenesis

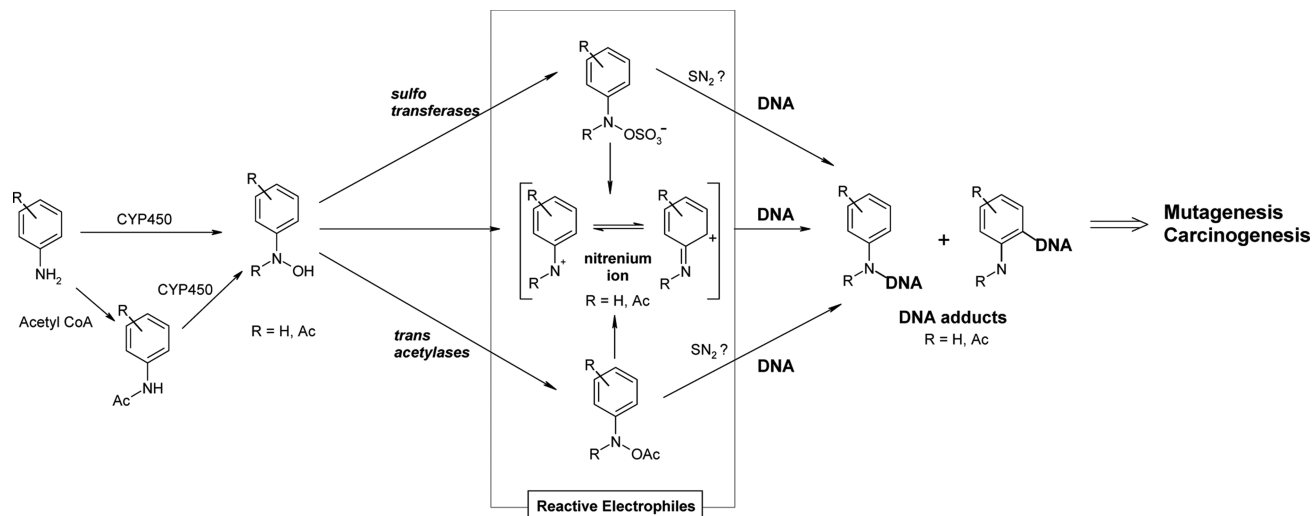


Table 8. Replacement of the Aniline Fragment: Mutagenicity Data

Aniline replacement		Insertion of ortho -substituents	
Fragment tested	Mutagenicity ^a	Fragment tested	Mutagenicity ^a
20h	Yes	20z	No
20w	No	20aa	No
20x	No	20aj	Yes
20ag	Yes	20ai	Yes
20y	No	20ab	No
20ah	Yes	20ac	No
20ad	NA		
20ae	No		
20af	No		

^aMeasured using the Ames II *Salmonella* assay in the presence of S9 fractions (all compounds were found “not mutagenic” without S9 fractions).

parameters are measures of the chemical reactivity, hence of the ability of undergoing oxidative metabolic transformations. Electron releasing substituents on the aromatic amine increase the electronic density on the aniline nitrogen, making it more susceptible to oxidation, polarize the hydroxylamine bond, favoring its heterolytic cleavage, and stabilize the nitrenium ion formed thus increasing the risk of mutagenicity. Having this in

mind, we built a MedChem plan aiming to identify new and safe chemical fragments in replacement of the mutagenic aniline.

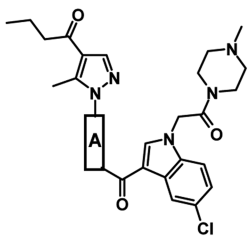
The insertion of nitrogen atoms within the aryl group was performed with the objective to decrease the lipophilicity of the fragment (Table 8, compounds 20w, 20x, 20y, and 20ag). 3-Aminopyridine 20ag was found to be mutagenic, while

Table 9. Replacement of the Aniline Fragment: (a) In vitro Biological Activities of Compounds Not Bearing a Mutagenic Fragment and (b) Human Antiaggregant Activity and eADME Parameters of Compounds 52w, 52z, 52ad, and 52ae

(a)

Cpd	A	Bnd ^a (nM)	Rat AA ^b (μM)	EF ^c
52w		17	0.06	2,6
-		Chemically unstable		
52y		275	1.3	358
52ad		40	0.15	6
52ae		7	0.02	0,6
52af		480	3.3	1584
52z		48	0.4	19
52aa		75	9.6	720
52ab		266	1.5	399
52ac		559	9.3	5199

(b)



Cpd	A	Human AA ^d (μM)	%metabolism (h,r,m) ^e	Caco2 ^f	<i>in vitro</i> intrinsic metabolic clearance (Cl_{int}) ^g (% CYP3A4 contribution)
52w		0.10	29 – 11 – 4	8	0.085 (43%)
52z		0.28	61 – 18 – 8	33	0.143 (67%)
52ad		0.10	73 – 32 – 11	1	0.171 (64%)
52ae		0.02	59 – 13 – 3	1	0.050 (35%)

^aP2Y12 binding ($n = 2$). ^bADP-induced platelet aggregation ($n = 2$, [ADP] = 2.5 μM) in rat platelet rich plasma. ^cEligibility factor = Bnd (nM) × AA in rPRP (μM). ^dADP-induced platelet aggregation ($n = 2$, [ADP] = 2.5 μM) in human platelet rich plasma. ^eIncubation with hepatic microsomal fractions during 20 min in the presence of 1 mM NADPH (e.g., 29% metabolism means for 71% of unchanged compound). ^fPermeability measured on a Caco2 cell monolayer, expressed in 10⁻⁷ cm·s⁻¹. ^g*In vitro* metabolism using human hepatocytes (incubation of 24 h), expressed in mL·h⁻¹·10⁶ hep⁻¹.

aminopyridazine, 2-aminopyridine, and aminopyrazine derivatives were not. Hence, the proximity of the N atom to the amino group seemed mandatory. The aminothiazole **20ah** which might be considered as an 2-aminopyridine bioisoster was found to be mutagenic. We did not find any correlation between mutagenicity and calculated physicochemical parameter for these five fragments. The replacement of the phenyl group of **20h** by a *trans*-cyclohexyl (**20ad**) or a piperidine motif (**20ae**) obviously prevented mutagenicity from the mechanisms described at Scheme 1. **20ad** is an aliphatic amine and was not tested in the Ames assay. As some hydrazine derivatives were described in the literature to be mutagenic,²¹ **20ae** was challenged in the Ames II assay and was found to be negative both with and without metabolic activation. Aniline replacement by a phenol group produced the nonmutagenic **20af** fragment. **20ac** was prepared as a bulky secondary amine that was indeed not found to be mutagenic. The insertion of ortho-substituents aiming to modulate both the polarity and the oxidability of the aniline fragment was done. Polar and/or electron withdrawing substituents such as nitrile (**20z**), carboxylic acid (**20aa**), or primary carboxamide (**20ab**) allowed prevention of mutagenicity, while the somehow lipophilic chlorine atom insertion (**20aj**) produced a mutagenic aniline. **20ai** was found to be mutagenic, while **20ab** was not. This may be due to the role played by the two methyl groups which increase the electronic density on the aromatic system together with the lipophilicity. At this stage, we were pleased to have in hand 10 new nonmutagenic fragments that were all engaged in the total synthesis of P2Y12 antagonists **52w** to **52af** (Table 9a). The synthesis of the 2-aminopyridine-containing final

derivative was not completed because in that specific case, the central amide linker appeared to be sensitive in slightly acidic and basic conditions. Five compounds out of nine (Table 9a, **52y**, **52aa**, **52ab**, **52ac**, and **52af**) were found to be inactive in both Bnd and rat AA assays. The four remaining compounds containing pyridazine (**52w**), *o*-benzonitrile (**52z**), *trans*-cyclohexyl (**52ad**), or piperidine (**52ae**) motifs, were elected for being evaluated further, as they displayed EF values below 20. It must be noted that this optimization aiming to replace the mutagenic aniline fragment was also very successful in terms of *in vitro* biological activity. Indeed, **52w** and **52ae** were the best methylpiperazine-containing compounds tested throughout the project, with respective EF values of 2.6 and 0.6 (Table 9a). As already observed with piperazine-containing actives, there was no discrepancy between human and rat functional activities (Table 9b). With IC₅₀ values below 100 nM, **52w**, **52ad**, and **52ae** are by far the most potent *in vitro* P2Y12 antagonist ever described in the literature. The four selected compounds were shown to be stable on rat and mouse microsomes. However, **52z**, **52ad**, and **52ae** displayed high levels of oxidative metabolism on human microsomes. These results were well correlated with the high clearance on human hepatocytes measured for **52z** and **52ad** (0.143 and 0.171 mL/h, respectively). Interestingly, **52ae** was much less cleared than expected (0.050 mL/h) and was finally selected on these criteria as well as **52w** that was found fine on human microsomes and hepatocytes. Additionally, the contribution of CYP3A4 to the hepatic clearance was found to be low for both compounds. Despite low permeations measured on Caco2 cells, we decided to perform a dose–response study with **52w**

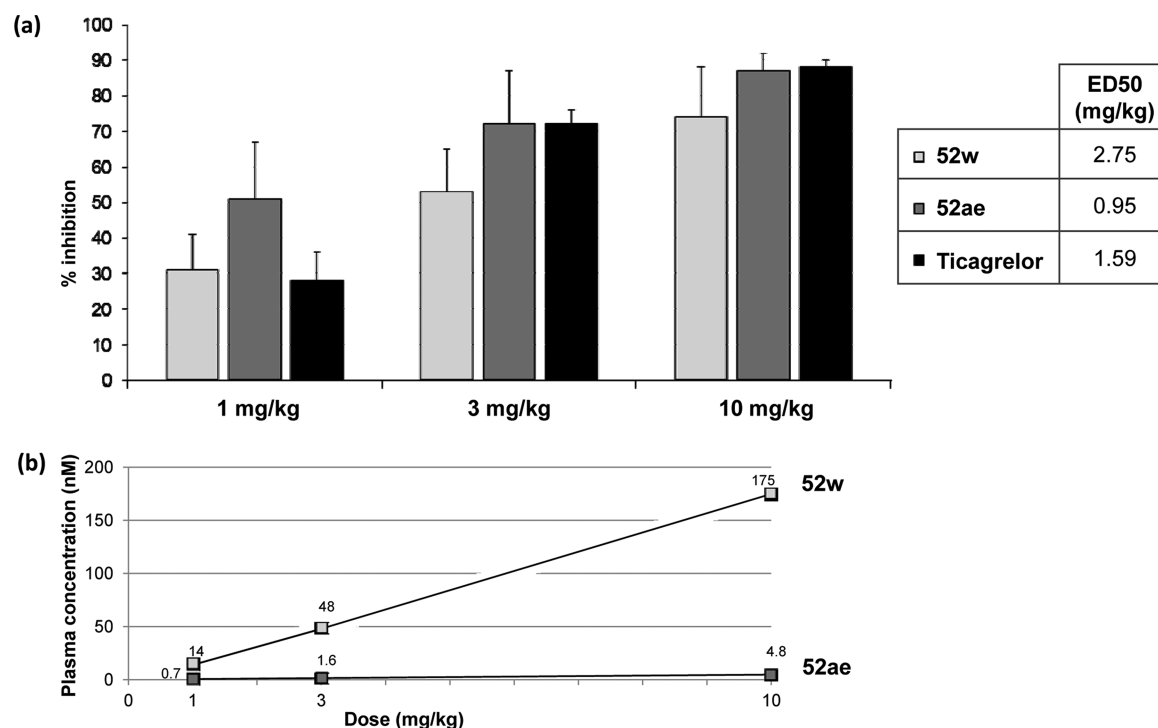


Figure 6. Dose–response study: (a) ex vivo inhibition of platelet aggregation in rats 2 h after oral dosing with 1, 3, and 10 mg/kg 52w, 52ae, and ticagrelor; (b) plasma concentrations measured for 52w and 52ae in the corresponding ex vivo experiment.

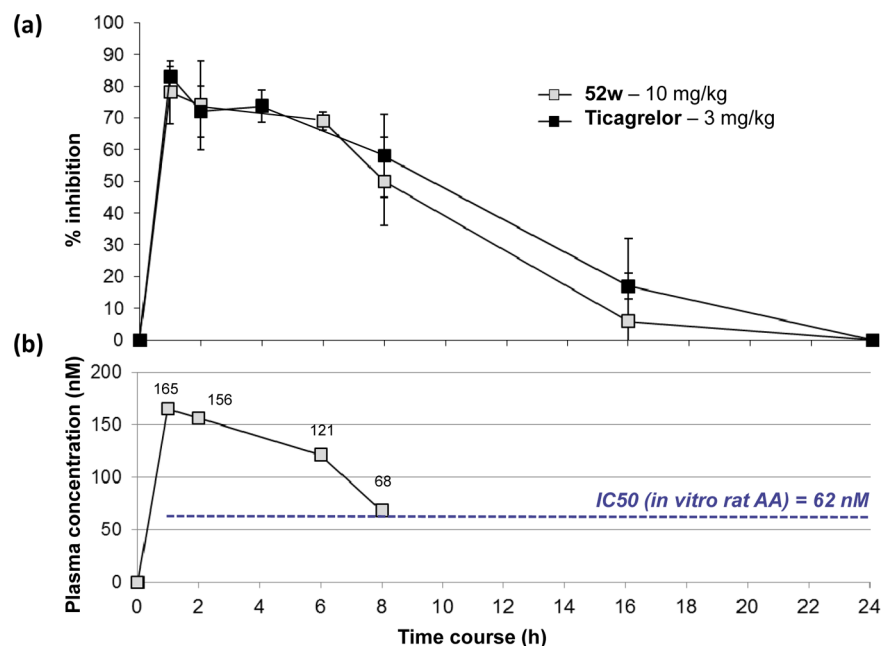
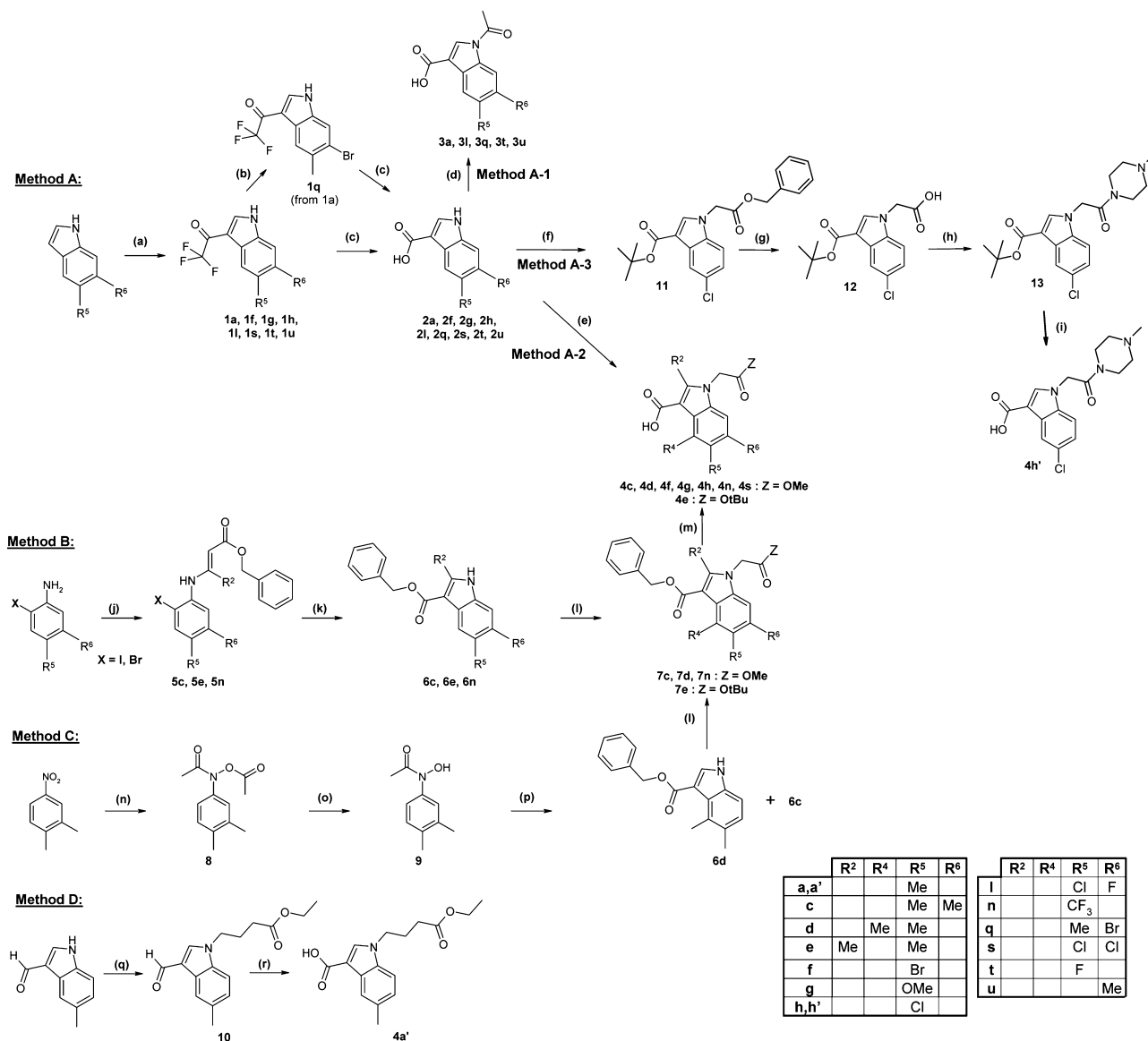


Figure 7. Kinetic study: (a) ex vivo inhibition of platelet aggregation in rats over time after oral dosing of 10 mg/kg 52w and 3 mg/kg ticagrelor; (b) plasma concentrations measured for 52w in the same ex vivo experiment.

and 52ae in our ex vivo platelet aggregation model in rats (Figure 6a). This was done in comparison with ticagrelor, 2 h after dosing. 52w and 52ae inhibited ADP-induced platelet aggregation in a dose-dependent manner with ED₅₀ values of 2.75 and 0.95 mg/kg, respectively. Nearly complete inhibition of platelet aggregation (85%) was observed with 52w at 30 mg/kg (data not shown). 52ae retained a significant level of activity at very low dose (~50% at 1 mg/kg), thus making it a very potent antiplatelet agent. Ticagrelor exhibited an ED₅₀ of 1.59

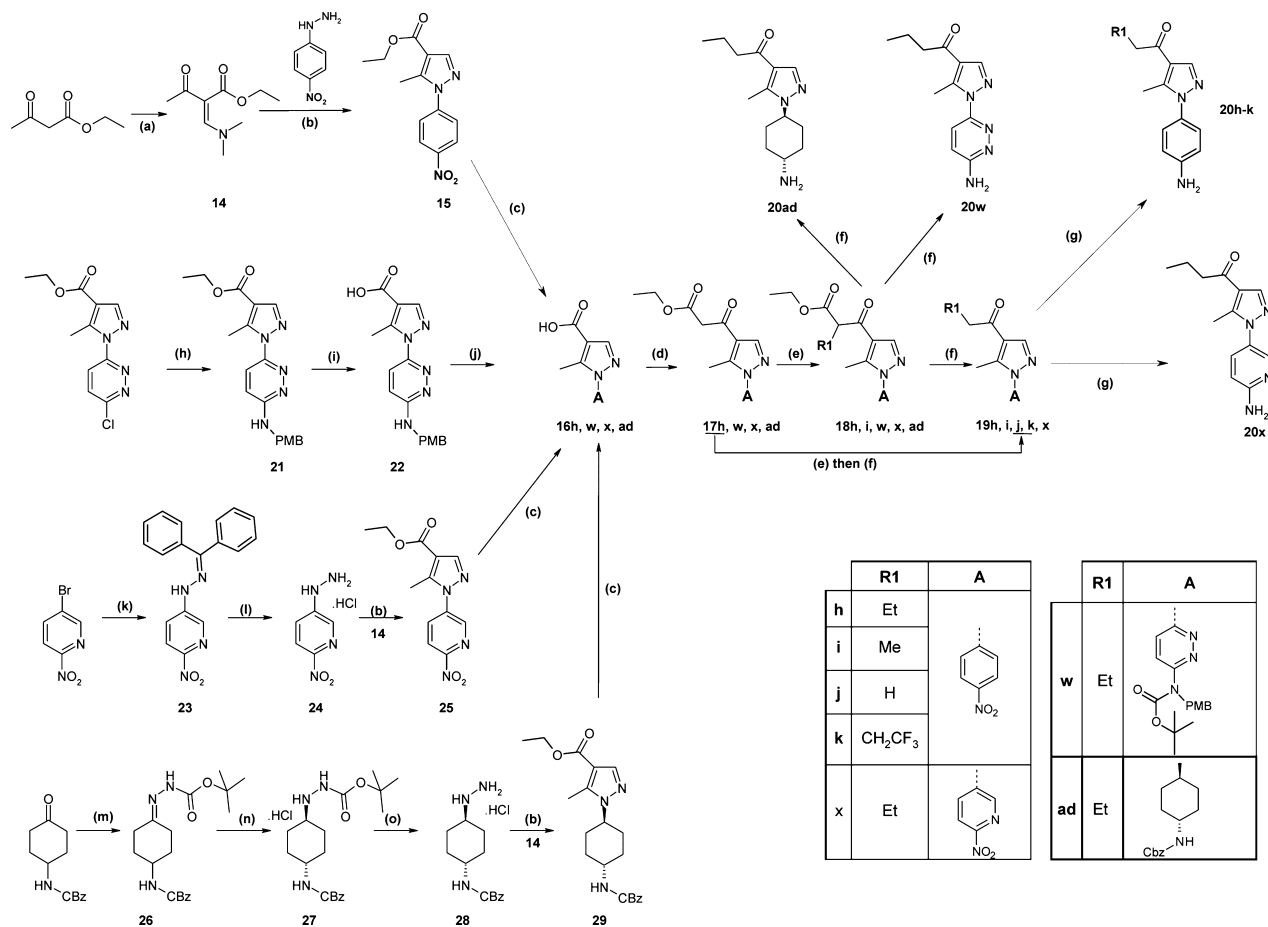
mg/kg, while clopidogrel and prasugrel displayed ED₅₀ values of 2.60 and 0.46 mg/kg in the same conditions, respectively.²² Plasma concentrations were determined from samples collected during this dose–response study. In the case of 52w, the circulating levels were very well correlated with both the level of antiaggregating activity and the dose (Figure 6b). On the other hand, the ex vivo activity of 52ae appeared to be high regarding the very low drug plasma concentrations. This kind of PK/PD profile may suggest a covalent mode of binding to the

Scheme 2. Synthesis of Key Substituted 3-Carboxyindoles 3 and 4^a

^a(a) (CF₃CO)₂O, diethyl ether, -5 °C, 83–99%; (b) Br₂, AcOH, rt, 81%; (c) KOH in H₂O, reflux, 62–99%; (d) Et₃N, DMAP, acetyl chloride, DCM, rt, 56–98%; (e) NaH (2 equiv), DMF, -10 °C to rt, then methyl bromoacetate, -20 °C to rt, 61–92%; (f) dimethylformamide di-*tert*-butylacetal, benzene, reflux, then benzyl bromoacetate, cesium carbonate, DMF, rt, 66% for two steps; (g) LiOH, THF/H₂O, 0 °C, quantitative; (h) EDC·HCl, pentafluorophenol, DMF, rt, then *N*-ethylmorpholine, 1-methylpiperazine, rt, 58%; (i) TFA, DCM, rt, quantitative. (j) For R² = H: LiCl, [1,4]benzoquinone, Pd(OAc)₂ cat., benzyl acrylate, THF, rt, 51–98%. For R² = Me: APTS, 3-oxobutyric acid benzyl ester, toluene, reflux in a Dean–Stark apparatus, 88%. (k) For R² = H: 1,4-diazabicyclo[2,2,2]octane, Pd(OAc)₂ cat., DMF, 120 °C, 22–70%. For R² = Me: tri(*o*tolyl)phosphine, Et₃N, Pd(OAc)₂ cat., acetonitrile, 140 °C under microwave, 97%. (l) K₂CO₃, methyl- or *tert*-butyl bromoacetate, DMF, rt, 96–98%; (m) Pd/C cat., ammonium formate, MeOH, reflux, 58–88%; (n) Pd/C, NH₂NH₂·H₂O, cyclohexane, 0 °C, then Et₃N, acetyl chloride, 10 °C, 37%; (o) K₂CO₃, MeOH, rt, 80%; (p) DMAP, propynoic acid benzyl ester, THF, 0 °C, then aq NaOH, rt, 40% (6c, 29%); (q) ^tBuOK, Br(CH₂)₃COOEt, DMF, rt, 90%; (r) 2-methyl-2-butene, NaClO₂, NaH₂PO₄, H₂O/THF/^tBuOH, 0 °C to rt, 88%.

receptor or the formation of hyperactive metabolites, the latter option seeming unlikely as 52ae was shown to be stable on rat microsomes (Table 9). These uncertainties around 52ae, especially regarding the initial specifications we had implemented (*reversible* and *directly acting* P2Y₁₂ antagonist), did not encourage us to move further in its *in vivo* characterization, and we decided to focus on compound 52w. 52w was also found to be active in this *ex vivo* model after *iv* administration (5 min after injection, I% (0.1 mg/kg) = 37 ± 22, I% (0.3 mg/kg) = 63 ± 10, I% (1 mg/kg) = 75 ± 7, I% (3 mg/kg) = 86 ± 2, and I% (10 mg/kg) = 92 ± 6).

As a next step, we performed a kinetic study after a 10 mg/kg oral administration of 52w that resulted in a rapid maximal inhibition of platelet aggregation (less than 1 h, Figure 7a). The extent of inhibition was maintained at relatively constant levels during several hours with an average percent of platelet inhibition of 74% during the first 6 h. Again, a high correlation was found between the extent of *ex vivo* inhibition of ADP-induced platelet aggregation and the circulating levels of 52w over time ($r = 0.861$, data not shown).²² Very interestingly, the *ex vivo* potency of 52w to inhibit ADP-induced platelet aggregation was also in excellent correlation with its *in vitro*

Scheme 3. Synthesis of Synthons 20h–k, 20w, 20x, and 20ad^a

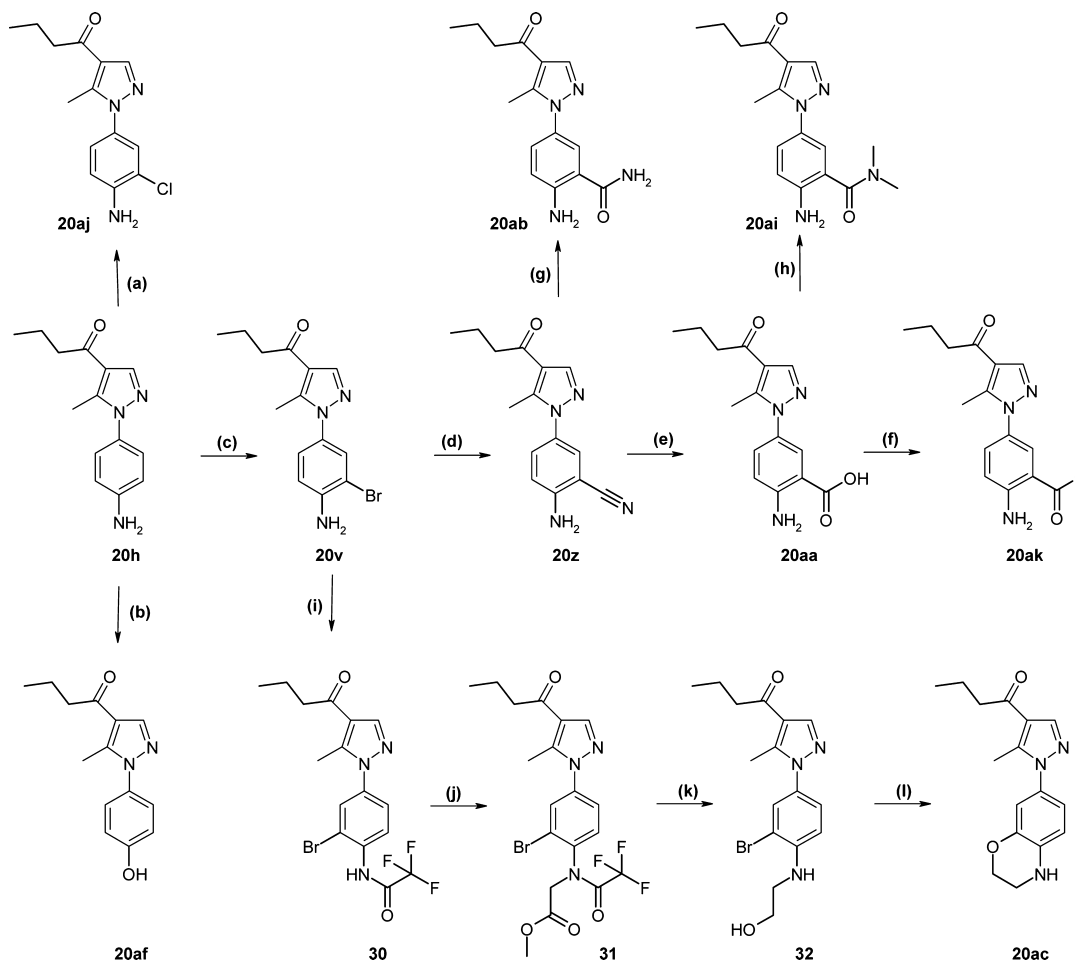
^a(a) DMF–DMA, 2 **h, rt, 99%; (b) EtOH, reflux, 2 h, 72–76%; (c) LiOH or NaOH or KOH, THF/EtOH/H₂O, reflux, 74–99%; (d) CDI, THF, rt, 20 h, then magnesium bis(3-ethoxy-3-oxopropanoate), 55 °C, 59–92%; (e) NaH 60%, THF, 0 °C then R₁X, rt, 24 h, 82–96%, or K₂CO₃, TBAB, R₁X, THF, 55 °C, 82–97%, or Cs₂CO₃, EtI, DMF, rt, 99%; (f) Aqueous HCl 37%, reflux, 2 h, 78–100%, or Al₂O₃, 1,4-dioxane/H₂O, 100 °C, 82%; (g) Pd/C, cyclohexene, EtOH, reflux, 57–95%, or H-Cube, EtOAc/MeOH, 57%; (h) 4-methoxybenzylamine, 1,4-dioxane, reflux, 2 h, 72%; (i) KOH, EtOH, 80 °C, 2 h, 98%; (j) DMAP, Et₃N, di-*tert*-butyl dicarbonate, DMF, rt, then aqueous KOH, rt, 56%; (k) Pd(OAc)₂, Cs₂CO₃, MePhos, benzhydrylidenehydrazine, ^tBuOH, 80 °C, 74%; (l) aqueous HCl 37%, rt, 72%; (m) *tert*-butyl carbazate, MeOH, rt, quant; (n) NaBH₃CN, AcOH/H₂O, rt, then HCl in EtOAc, rt, 63%; (o) HCl 4 M in 1,4-dioxane, rt, 90%.

potency in rats (IC₅₀ = 62 nM, Figure 7b). A nearly identical profile of ex vivo inhibition was observed with ticagrelor in the same experimental conditions at a 3 mg/kg oral dose (Figure 7a) which was in good correlation with its plasma circulating levels ($r = 0,836$).²² By contrast, its ex vivo activity was not consistent with its in vitro potency (AA in rPRP, IC₅₀ = 4160 nM), thus suggesting that ticagrelor may exert its activity through complementary mechanisms of action independent of its ability to antagonize P2Y₁₂ receptors. A preclinical study in a rat shunt thrombosis model demonstrated a dose-dependent antithrombotic activity after oral administration of **52w** together with a favorable safety profile as demonstrated in a rat tail bleeding model.²²

52w has demonstrated an excellent selectivity (IC₅₀ > 10 μM) against a large panel of receptors, enzymes, and ion channels (see Supporting Information).²² No toxicity was achieved and no damaged target organ identified in a 7-day oral (30 and 100 mg/kg) and intravenous (3 and 10 mg/kg) toxicity study in rats. In this study the plasma exposure was found to be in the same range after a single as well as after a 7-day repeated administration (AUC_(0–24)(day 7)/AUC_(0–24)(day 1) ratio of 1.3), suggesting the absence of autoinduction or

accumulation process. In addition, **52w**, orally administered at the 100 mg/kg dose to conscious telemetered mongrel dogs, did not induce any major hemodynamic or electrocardiographic effects and did not affect body temperature within 24 h after treatment. Mean maximal plasma concentration measured 4 h after dosing reached 2340 ± 388 ng/mL (4.2 μM).

Preparation of Compounds. (Code numbers are given at Table 1.) Depending on the commercial availability of starting materials, synthons **3** and **4** were prepared following four different methods described in Scheme 2 (methods A–D). Method A was the most convenient, as it allowed getting most of synthon **3** or **4**, starting from commercially available 5,6-substituted indoles. The first two steps were adapted from a previously published work and consisted of the selective trifluoroacetylation at position 3 using trifluoroacetic anhydride in diethyl ether, thus producing intermediates **1** followed by the forced hydrolysis of the trifluoroacetyl group to produce compounds **2**.²³ **1q** was obtained after bromination of **1a**. Acetylation of intermediates **2** in mild conditions led to compounds **3a**, **3l**, **3q**, **3t**, and **3u** (method A-1), while activation with 2 equiv of NaH followed by the thermodynamically controlled *N*-indole substitution with 1 equiv of methyl

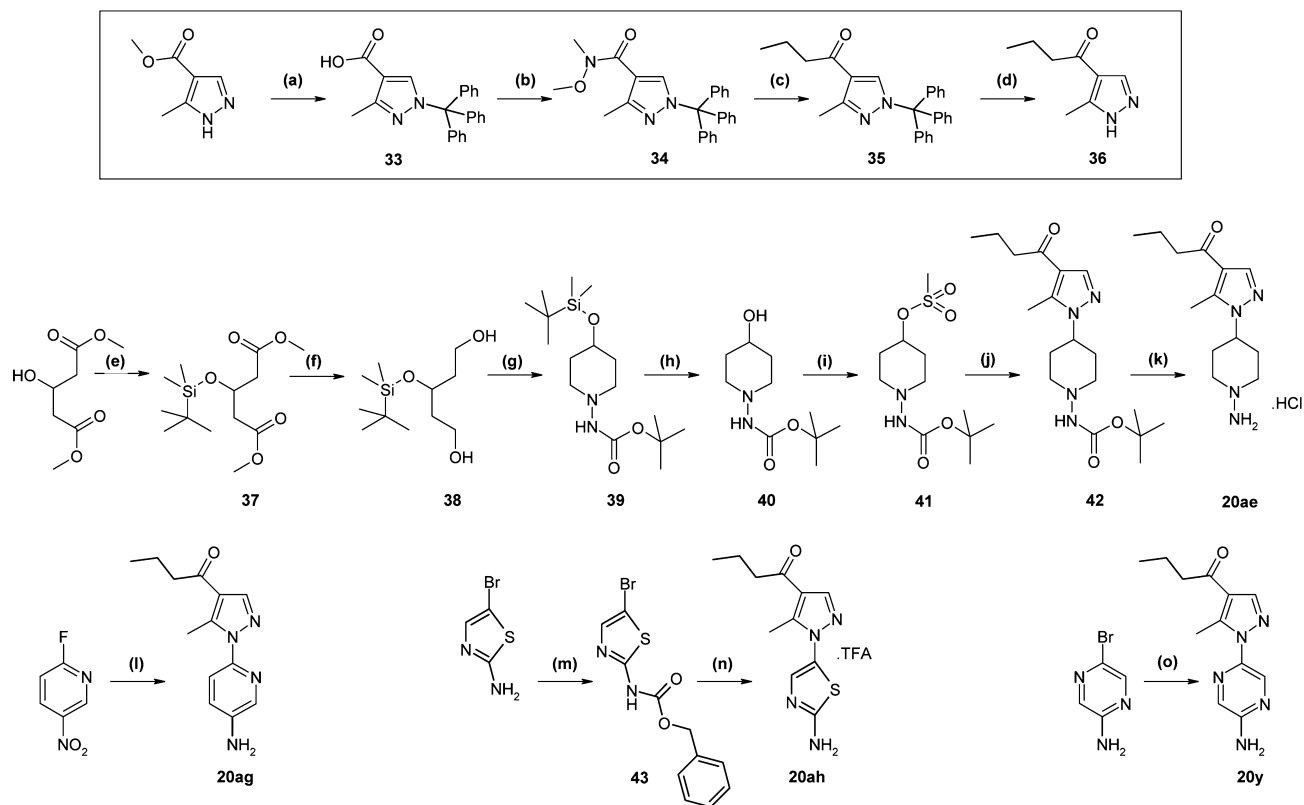
Scheme 4. Synthesis of Compounds 20v, 20z, 20aa, 20ab, 20ac, 20af, 20ai, 20aj, and 20ak^a

^a(a) NCS, acetonitrile, reflux, 88%; (b) H₂SO₄, NaNO₂, H₂O, 0 °C to reflux, 80%; (c) NBS, acetonitrile, reflux, 76%; (d) ZnCN₂, Pd(PPh₃)₄, DMF, 100 °C, 85%; (e) NaOH, H₂O, reflux, 87%; (f) KHCO₃, CH₃I, DMF, rt, 87%; (g) NaOH, 1,4-dioxane/H₂O, 100 °C, 66%; (h) N-methylmorpholine, BOP, DCM, rt, then Me₂NH·HCl, rt, 58%; (i) (CF₃CO)₂O, DCM, rt, 97%; (j) NaH 60%, THF, 0 °C, then methyl bromoacetate, rt, 99%; (k) K₂CO₃, MeOH, then aq 2 N NaOH, then CDI, Et₃N, THF, then NaBH₄, rt, 37%; (l) Cs₂CO₃, 2-(di-*tert*-butylphosphino)-1,1'-binaphthyl, Pd(OAc)₂, toluene, 70 °C, 68%.

bromoacetate produced compounds **4f**, **4g**, **4h**, and **4s** (method A-2). It was very interesting to note here that this original regiocontrolled addition prevented a sequence of cumbersome protection/deprotection steps. Alternatively, compound **4h'** was prepared starting from compound **2h**, through a sequence of protection/alkylation with benzyl bromoacetate/deprotection steps (compounds **11** and **12**) followed by the methylpiperazine insertion (**13**) and *tert*-butyl ester deprotection (method A-3). This **4h'** synthon was very promising, as it gave the potential to go directly to final methylpiperazine-containing compounds **52**. This method was used to produce compound **52ae** (Scheme 6). Unfortunately, **4h'** was not stable enough in the stronger reaction conditions required to couple aromatic amines, and this method could not be generalized. Method B was already described in the literature and provided compounds **4** from correctly substituted anilines.²⁴ Commercially available *o*-halogenoanilines were engaged in a Pd-catalyzed reaction with benzyl acrylate to form compounds **5c** and **5n**. **5e** was prepared from 2-bromo-4-methylphenylamine and 3-oxobutyrac acid benzyl ester in the presence of *p*-toluenesulfonic acid. Compounds **5** were then submitted to a Pd-catalyzed cyclization, thus producing compounds **6c**, **6e**, and **6n**. Method C is another option, allowing the generation of

the fully acetylated *N*-hydroxylamine **8** from the corresponding nitro derivative. It was followed by a selective O-deacetylation to afford **9**, which was then submitted to a one step Pd-catalyzed addition/cyclization with benzyl propionate to form **6d**.²⁵ In the absence of ortho substituents, the cyclization was allowed at both sides, thus additionally producing the **6c** isomer. Compounds **7** were the point of convergence of methods B and C and were obtained by alkylation with alkyl bromoacetates. Finally, a catalytic hydrogenation over Pd/C produced the key synthons **4c**, **4d**, **4e**, and **4n**. The very first method we used to produce 5-methylindole derivatives was from indole-3-carbaldehyde, a nonreactive precursor of the indole-3-carboxylic acid motif. Thus, this allowed the straightforward *N*-alkylation with ethyl 4-bromobutyrate producing **10**, followed by aldehyde oxidation using the sodium chlorite and 2-methylbut-2-ene couple to form **4a'** (method D).²⁶

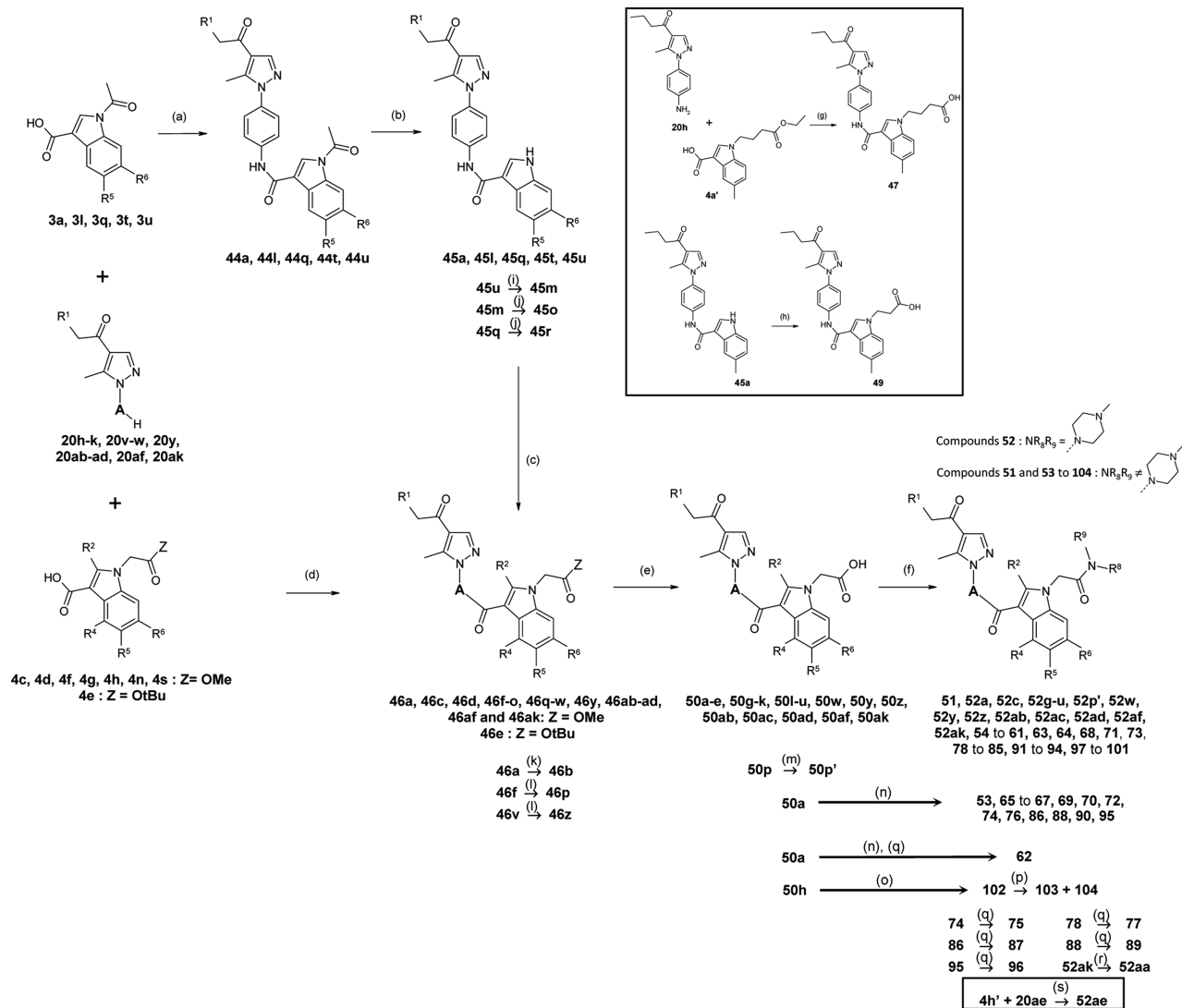
Compounds **20h–k**, **20w**, **20x**, and **20ad** were prepared following a chemical strategy that was already described in the literature to produce a large variety of alkyl ketones from carboxylic acid derivatives (Scheme 3).²⁷ The common 4-carboxypyrazole scaffold of **16h**, **16w**, **16x**, and **16ad** is key in this synthetic method. **16h** was prepared in three steps from 3-

Scheme 5. Synthesis of Synthons 20y, 20ae, 20ag, and 20ah^a

^a(a) K_2CO_3 , TrCl, DMF, rt, then KOH, EtOH/H₂O, 56%; (b) DMAP, BOP-Cl, DCM, then *N,O*-dimethylhydroxylamine hydrochloride, rt, 87%; (c) *n*-PrMgCl, THF, $-30\text{ }^\circ\text{C}$ to rt, 85%; (d) HCl 4 M in 1,4-dioxane, rt, 62%; (e) TBDMSCl, imidazole, DCM, rt, 82%; (f) $LiBH_4$, diethyl ether, rt, quantitative; (g) oxalyl chloride, DMSO, DCM, $-78\text{ }^\circ\text{C}$, then Et_3N , $0\text{ }^\circ\text{C}$, then *tert*-butyl carbazate, $NaBH(OAc)_3$, DCM, $0\text{ }^\circ\text{C}$, 51%; (h) TBAF, THF, $0\text{ }^\circ\text{C}$ to rt, 78%; (i) DMAP, Et_3N , $MeSO_2Cl$, DCM, rt, quantitative; (j) 36, $tBuOK$, DMF, $50\text{ }^\circ\text{C}$, 10%; (k) TFA, DCM, rt, 80%; (l) 36, NaH 60%, DMF, rt, then Pd/C, H₂ (2 bar), THF, rt, 26% for two steps; (m) pyridine, benzyl chloroformate, acetonitrile, rt, 93%; (n) 36, K_2CO_3 , CuI, *trans*-*N,N'*-bismethyl-1,2-cyclohexane diamine, $85\text{ }^\circ\text{C}$, then TFA, reflux, 11% for two steps; (o) 36, K_2CO_3 , proline, CuI, DMSO, $130\text{ }^\circ\text{C}$, 18%.

oxobutyric acid ethyl ester. A first condensation between *N,N*-dimethylformamide dimethyl acetal and 3-oxobutyric acid ethyl ester produced 14. A second condensation with (4-nitrophenyl)hydrazine led to 15 that was further hydrolyzed to afford 16h. 16w was obtained in three steps from its chloropyridazine analogue.²⁸ Reaction with *p*-methoxybenzylamine as the solvent at high temperature produced 21 which was then hydrolyzed to form the carboxypyrazole 22. Finally, as we did not succeed in elongating the carboxylic acid of 22, the secondary aromatic amine was Boc-protected to afford 16w. 16x was obtained in four steps from commercially available 5-bromo-2-nitropyridine that was first reacted with benzhydrylidenehydrazine under Pd(II) catalysis (23) followed by HCl deprotection to produce 24 in its hydrochloride form. Condensation with 14 afforded pyrazole 25 that was then hydrolyzed to give 16x. 16ad was obtained in five steps from (4-oxocyclohexyl)carbamic acid benzyl ester that was first condensed with *tert*-butyl carbazate to produce 26. The reduction of 26 using sodium cyanoborohydride in acidic conditions produced the racemic *cis/trans* hydrazine mixture. Very interestingly, the pure *trans* isomer 27 was isolated in its hydrochloride form by precipitation upon addition of an organic HCl solution to the racemic mixture dissolved in EtOAc. Then Boc removal in HCl/1,4-dioxane (28) was followed by condensation with 14, leading to 29 which was hydrolyzed to afford 16ad. The elongation of the 4-carboxypyrazole derivatives 16h, 16w, 16x, and 16ad was performed using a

magnesium salt of 3-ethoxy-3-oxopropanoate, leading to compounds 17h, 17w, 17x, and 17ad, respectively. The activation of the malonate proton with sodium hydride allowed the insertion of various alkyl groups through reaction with halogenoalkanes (compounds 18h, 18i, 18w, 18x, and 18ad), followed by a decarboxylation/deprotection step in strong acidic conditions producing compounds 19h, 19i, 19x, 20w, and 20ad. The reaction of 17h with 1,1,1-trifluoro-2-iodoethane was not complete. The purification appeared to be difficult because of the coelution of the expected product and the starting material on silica gel. Therefore, the decarboxylation step was performed on the crude, leading to a mixture of 19j and 19k which were easily separated on silica gel. Key intermediates 20h, 20i, 20j, 20k, and 20x were obtained by reduction of the nitro group using Pd/C either in batch with cyclohexene as the source of hydrogen or with the H-cube apparatus that generates molecular hydrogen in situ from the electrolysis of water under flow conditions. 20h was a key intermediate, as it allowed the preparation of a variety of aniline derivatives (Scheme 4). Ortho-halogenation using *N*-chloro- or *N*-bromosuccinimide led to 20aj and 20v, respectively. Preparation of the diazonium ion from 20h followed by heating in water produced phenol 20af. Trifluoroacetylation of 20v (30) followed by insertion of a methyl acetate chain led to 31. Trifluoroacetyl removal, methyl ester hydrolysis, and reduction of the activated carboxylic acid using $NaBH_4$ afforded the alcohol 32, which was then engaged in a Pd(II)-catalyzed

Scheme 6. Synthesis of Compounds 44–47 and 49–104^a

^a(a) DMAP, 0 °C, then EDC-HCl, DCM, rt, 28–98%; (b) K₂CO₃, MeOH, rt, 30–89%; (c) K₂CO₃, methyl bromoacetate, DMF, rt, 42–95%; (d) EDC-HCl, DMAP, 1,2-dichloroethane, rt, 11–96% or SOCl₂, DMF cat., DCM, reflux then 4 Å molecular sieves, DMAP, 1,2-dichloroethane, 80 °C, 24–72%; (e) aq NaOH, MeOH or 1,4-dioxane or MeOH/1,4-dioxane or THF, rt, 41–98%, or (46ak → 50ak) aq LiOH, THF, rt, 68%, or (46e → 50e) TFA, DCM, rt, 25%; (f) HNR₈R⁹, Et₃N, BOP-Cl, DCM, rt, 15–97%, or Excess HNR₈R₉, BOP-Cl, DCM, rt, 17–95%, or Excess HNR₈R₉, pyridine, BOP-Cl, DMF, rt, 69%; (g) Et₃N, BOP-Cl, DMF, 50 °C, then aq NaOH in MeOH, rt, 29%; (h) ethyl acrylate, benzyltrimethylammonium hydroxide, 1,4-dioxane, then aq NaOH, rt, 25%; (i) Br₂, AcOH, rt, 41%; (j) NiCl₂, DMF, 200 °C under microwave, 73–80%; (k) NaH, DMF, 4 °C, then CH₃I, rt, 27%; (l) ZnCN₂, Pd(PPh₃)₄, DMF, 100 °C in a sealed tube, 82–84%; (m) AcOH/aq 35% HCl, 90 °C, 44%; (n) Boc-protected HNR₈R⁹, Et₃N, BOP-Cl, DCM, rt, then HCl in 1,4-dioxane/EtOAc/MeOH, rt, 15–89%; (o) piperazine-2-carboxylic acid methyl ester, Et₃N, BOP-Cl, DCM, rt, then *tert*-butyl methyl(2-oxoethyl)carbamate, sodium cyanoborohydride, AcOH, MeOH, rt, then TFA, rt, then aq NaOH, 57%; (p) separation on a chiral column using supercritical conditions; (q) K₂CO₃, CH₃I, DMF, rt, 13–78%; (r) aq LiOH, THF, rt, 60%; (s) diisopropylethylamine, HOBt, EDC-HCl, DMF, rt, 33%.

cyclization step to form the morpholine motif of 20ac. 20v was also the starting point leading to 20z through a Pd(II)-catalyzed cyanation. Mild hydrolysis of 20z produced the primary carboxamide 20ab, while stronger hydrolysis conditions led to the carboxylic acid 20aa, which was either coupled with dimethylamine to form 20ai or methylated to afford ester 20ak.

Another key synthon is pyrazole 36 which was prepared in four steps from 5-methyl-1H-pyrazole-4-carboxylic acid methyl ester (Scheme 5). Trityl insertion followed by methyl ester hydrolysis led to 33 which was then activated through the formation of the corresponding Weinreb amide 34. Reaction with *n*-propylmagnesium chloride (35) followed by trityl

removal produced compound 36. Intermediate 20ae was prepared in seven steps from 3-hydroxypentanedioic acid dimethyl ester. Silylation (37) followed by ester reduction with lithium borohydride produced 38. Alcohol oxidation under Swern conditions followed by a double reductive amination with *tert*-butyl carbazate in the presence of sodium triacetoxyborohydride afforded 39. TBDMS removal (40) followed by alcohol activation led to mesylate 41 which was reacted with 36 to produce 42. Reaction yield was low, as the formation of the position isomer was sterically favored (alkylation at the second pyrazole nitrogen). TFA-mediated BOC-deprotection finally afforded compound 20ae. Pyrazole 36 was also reacted with 5-

bromopyrazin-2-ylamine to afford **20y** or with (5-bromothiazol-2-yl)carbamic acid benzyl ester (**43**) to produce **20ah** or with 2-fluoro-5-nitropyridine to produce a nitropyridine intermediate that was then reduced to **20ag**.

Intermediates **3**, **4**, and **20** are the three key synthons for the preparation of compounds **44** and **45** (Scheme 6). Preparation of compounds **44** was done from synthons **20** and **3** using EDC·HCl as the coupling agent. Then acetyl removal with potassium carbonate in MeOH produced compounds **45a**, **45l**, **45q**, **45t**, and **45u**. Bromination of **45u** in AcOH afforded **45m**. Bromoaryl substitution by a chlorine atom was possible using NiCl₂ in DMF (**45o** from **45m** and **45r** from **45q**).²⁹ Then reaction with methyl bromoacetate produced compounds **46a**, **46l**, **46m**, **46o**, **46q**, **46r**, **46t**, and **46u**. Alternatively, other compounds **46** were prepared from corresponding synthons **20** and **4** (Scheme 6). Some intermediates **20** were not engaged in coupling for various reasons. **20ag**, **20ah**, **20ai**, **20aj** were not transformed in final compounds, as they were found to be mutagenic. **20x** was reacted. However, **46x**, the expected product of the reaction, was found to be unstable, and the synthesis was discontinued. Probably because of the electron withdrawing effect of the nitrile group, the amino group of **20z** was found to be totally nonreactive. Thus, **46z** was obtained from **46v**. The same palladium-catalyzed cyanation procedure was used to generate **46p** from **46f**. **46b** was produced from **46a** using the NaH/CH₃I couple in DMF. Compounds **50** were the result of the mild hydrolysis of carboxylic esters **46** using aqueous NaOH in organic solvents (Scheme 6). In the specific case of **46ak**, bearing also an aromatic methyl ester, aqueous LiOH was used to produce **50ak**. The *tert*-butyl ester from **46e** was reacted in TFA/DCM to produce **50e**. Mild nitrile hydrolysis of **50p** produced the corresponding carboxamide **50p'**. Alternatively, **47**, bearing a butanoic side chain, was prepared through a peptidic coupling between **20h** and **4a'** followed by ester hydrolysis, and **49**, bearing a propanoic side chain, was obtained by a Michael addition of **45a** with ethyl acrylate followed by ester hydrolysis (Scheme 6).

Usually, final compounds were prepared directly from compounds **50** through peptidic couplings (Scheme 6). Sometimes more than one step was necessary. Hence, the preparation of **53**, **65–67**, **69**, **70**, **72**, **74**, **76**, **86**, **88**, **90**, and **95** required a BOC-deprotection step after peptidic coupling, sometimes followed by a methylation step to produce **62**, **75**, **77**, **87**, **89**, and **96**. Compound **102** was the result of a sequence of four chemical steps from **50h** (Scheme 6). Peptidic coupling with piperazine-2-carboxylic acid methyl ester was followed by a reductive amination with *tert*-butyl methyl(2-oxoethyl)-carbamate. BOC deprotection in TFA followed by intramolecular cyclization upon basification produced **102** as a racemic mixture. Separation on a chiral column led to the two enantiomers **103** and **104**. Finally, mild hydrolysis of **52ak** using aqueous LiOH in THF afforded **52aa**.

CONCLUSION

In the search for a backup to clopidogrel, we initiated a HTS campaign designed to identify novel reversible P2Y₁₂ antagonists. Starting from a hit with low micromolar binding activity, we had set up a rational and sequential SAR optimization process leading to the identification of **52w**. The first sequence was focused on the optimization of the *in vitro* binding activity leading to **A₃** followed by the key finding of the pyrazole ketone motif as a metabolically stable pyrazole ester

surrogate in **A₄** (Figure 2). A clear breakthrough was the successful rescaffolding of an *o*-aminoanisole into an indole motif and the ensuing identification of compound **50a**. Carboxylic acid to carboxamide shift was also very decisive, as it allowed reaching submicromolar functional activities together with the limitation of species discrepancies. Carboxamide derivatives showed a much higher level of permeation on Caco2 cells which was promising as part of our aim to identify orally bioavailable compounds. After optimization, **52h** was identified that displayed a high level of *in vivo* antiplatelet activity. The last sequence of the optimization process, aiming to get rid of a mutagenic aniline fragment that we decided to avoid, led to **52w**. **52w** is a potent, highly selective, and reversible P2Y₁₂ receptor antagonist (binding, 17 nM; *in vitro* antiaggregant activity, 60 nM in rat and 100 nM in human). **52w** is directly active and does not require any metabolic activation which was a prerequisite set in stone from the beginning of the project. **52w** displays an ADME-T profile consistent with its MPK development. *Ex vivo* studies showed a rapid onset of action (within the first hour after oral administration) and a long duration of antiplatelet activity after either intravenous or oral administration. This duality in the mode of administration offered by **52w** is unique and gives an excellent opportunity for the intravenous treatment of acute coronary syndrome and the oral prevention of secondary thrombotic events which is a clear advantage compared to current standards of care. **52w** displays a potent antithrombotic activity in an arterial thrombosis model, with the best bleeding/antithrombotic balance when compared to clopidogrel, prasugrel, and ticagrelor.²²

Accordingly, **52w** has the potential to differentiate from other antiplatelet agents and was selected for development as the preclinical candidate SAR216471.

EXPERIMENTAL METHODS

Reactions were run using commercially available starting materials without further purification. All solvents were analytical grade, and anhydrous reactions were performed in oven-dried glassware under an atmosphere of argon or nitrogen. The microwave procedures were carried out with a Biotage microwave. The proton nuclear magnetic resonance spectra (¹H NMR) were recorded on Bruker spectrometers (250, 400, and 500 MHz) in DMSO-*d*₆ or CDCl₃. The chemical shifts δ were expressed in parts per million (ppm). The following abbreviations were used for interpreting the spectra: s, singlet; d, doublet; t, triplet; q, quadruplet; quint, quintuplet; sext, sextuplet; m, multiplet; dd, doublet of doublets; br, broad singlet. HPLC–UV–MS (liquid chromatography/UV detection/mass spectrometry) and melting points (mp) analyses were given hereafter only for compounds that were involved in biological assays. The UV purity of the compounds was assessed to be above 95%. Results of elemental analysis were obtained within $\pm 0.3\%$ of the theoretical values. Melting points were determined using open capillary tubes on a Buchi 530 apparatus and are uncorrected. The HPLC–UV–MS equipment used was composed of a chromatographic chain equipped with a diode array detector and a quadrupole mass spectrometer: Agilent 1100 series; Symmetry C18 3.5 μ m (2.1 mm \times 50 mm, Waters); solvent A, water + 0.005% TFA; solvent B, MeCN + 0.005% TFA; 0.4 mL/min, 25 °C; MSD SL (Agilent) ESI+.

Parameters for methods A and B are shown in Table 10.

Method C involved the following: Phenomenex Luna C18(2) column, 10 mm \times 2 mm, 3 μ m; gradient, water + 0.05% TFA/acetonitrile 93:7 (0 min) to 5:95 (1.20 min) to 5:95 (1.40 min); 1.1 mL/min, 30 °C; Agilent series 1100 MSD.

Chemical names of the molecules have been generated using ACDName, version 12, from Advanced Chemistry Development, Inc.

1-(5-Bromo-1H-indol-3-yl)-2,2,2-trifluoroethanone (1f). Tri-fluoroacetic anhydride (21.3 mL, 151 mmol) in diethyl ether (70 mL)

Table 10

gradient (min)	solvent A	solvent B
	Method A	
0	100	0
10	0	100
15	0	100
	Method B	
0	100	0
30	0	100
35	0	100

was added dropwise to a cold solution ($-5\text{ }^{\circ}\text{C}$) of 5-bromoindole (20 g, 101 mmol) in diethyl ether (250 mL). It was stirred for 2 h at $-5\text{ }^{\circ}\text{C}$. The precipitate formed was drained and washed with diethyl ether. **1f** was obtained as a white powder (24.5 g, 83%). $^1\text{H NMR}$, DMSO- d_6 (250 MHz), δ (ppm): 12.85 (br, 1H), 8.55 (s, 1H), 8.31 (s, 1H), 7.58 (d, $J = 8.8\text{ Hz}$, 1H), 7.50 (d, $J = 8.8\text{ Hz}$, 1H).

1-(5-Chloro-1H-indol-3-yl)-2,2-trifluoroethanone (1h). Same procedure was used as for **1f** (37.9 g, 93%). $^1\text{H NMR}$, DMSO- d_6 (250 MHz), δ (ppm): 12.89 (br, 1H), 8.58 (q, $J = 1.9\text{ Hz}$, 1H), 8.16 (d, $J = 2.1\text{ Hz}$, 1H), 7.63 (d, $J = 8.7\text{ Hz}$, 1H), 7.39 (dd, $J = 8.6, 2.1\text{ Hz}$, 1H).

5-Bromo-1H-indole-3-carboxylic Acid (2f). **1f** (24.0 g, 82.2 mmol) was added to a solution of potassium hydroxide (46.1 g, 822 mmol) in water (25 mL) and then heated for 4 h under reflux. The reaction mixture was cooled and washed with diethyl ether. The aqueous phase was cooled to $5\text{ }^{\circ}\text{C}$ and then neutralized with a solution of phosphate buffer preloaded with 35% hydrochloric acid. The precipitate formed was drained, washed with water, and dried under vacuum. **2f** was obtained as a white powder (15.6 g, 79%). $^1\text{H NMR}$, DMSO- d_6 (250 MHz), δ (ppm): 12.10 (br, 1H), 12.02 (br, 1H), 8.14 (d, $J = 1.9\text{ Hz}$, 1H), 8.06 (s, 1H), 7.46 (d, $J = 8.6\text{ Hz}$, 1H), 7.32 (dd, $J = 8.6, 1.9\text{ Hz}$, 1H).

5-Chloro-1H-indole-3-carboxylic Acid (2h). Same procedure was used as for **2f** (27.6 g, 92%). $^1\text{H NMR}$, DMSO- d_6 (250 MHz), δ (ppm): 12.10 (s, 1H), 11.95 (s, 1H), 8.07 (s, 1H), 7.97 (s, 1H), 7.49 (d, $J = 8.5\text{ Hz}$, 1H), 7.20 (d, $J = 8.5\text{ Hz}$, 1H).

5-Chloro-1-(2-methoxy-2-oxoethyl)-1H-indole-3-carboxylic Acid (4h). A solution of **2h** (10 g, 51.1 mmol) in DMF (110 mL) was added dropwise to a suspension of NaH (60% in oil, 4.50 g, 112.5 mmol) in DMF (400 mL) at $-10\text{ }^{\circ}\text{C}$. After it returned to room temperature, it was stirred for 1 h. The reaction mixture was cooled to $-20\text{ }^{\circ}\text{C}$. Methyl bromoacetate (4.86 mL, 51.1 mmol) was added dropwise, and then it was returned to room temperature for a period of 5 h and stirred for 15 h. The reaction mixture was added to 1 L of EtOAc/aqueous 1 N HCl mixture. The organic phase was collected, and the aqueous phase was extracted with EtOAc. The combined organic phases were washed with water and with brine, then dried over Na_2SO_4 and evaporated to dryness to afford **4h** as a white powder (8.9 g, 65%). $^1\text{H NMR}$, DMSO- d_6 (250 MHz), δ (ppm): 12.3 (br, 1H), 8.12 (s, 1H), 7.98 (s, 1H), 7.57 (d, 1H), 7.26 (d, 1H), 5.22 (s, 2H), 3.70 (s, 3H).

1-Benzyloxycarbonylmethyl-5-chloro-1H-indole-3-carboxylic Acid tert-Butyl Ester (11). To a solution of **2h** (5.00 g, 26.0 mmol) in benzene (200 mL) was added dimethylformamide di-*tert*-butyl acetal (25 mL, 104 mmol). The reaction mixture was refluxed for 12 h. After this time another portion of the acetal (25 mL) was added and the mixture stirred again under reflux for 12 h. It was concentrated, diluted with DCM, and washed three times with a saturated aqueous NaHCO_3 solution. To the crude product (5.7 g, 22 mmol) in solution in DMF (150 mL) were added benzyl bromoacetate (3.50 mL, 22.0 mmol) and cesium carbonate (11.1 g, 34.0 mmol). After the mixture was stirred for 12 h it was diluted with DCM and washed three times with an aqueous LiCl solution (4% w/w). The organic layer was dried over MgSO_4 and the crude product obtained after evaporation was purified by chromatography on silica gel, eluting with a gradient of EtOAc/MeOH to afford **11** (5.80 g, 66%). LCMS (method C): $M - \text{tBu} + \text{H}^+$ (t_R) = 344.2 (1.22 min).

1-Carboxymethyl-5-chloro-1H-indole-3-carboxylic Acid tert-Butyl Ester (12). To a solution of **11** (9.80 g, 24.4 mmol) in a mixture of THF/ H_2O (140 mL, 4/1; v/v), was added aqueous 2 N LiOH (12.2 mL, 24.4 mmol) at $0\text{ }^{\circ}\text{C}$. After the mixture was stirred for 3 h at this temperature, conversion was complete and the reaction mixture was adjusted to pH 6 by the addition of aqueous 1 N HCl. Upon evaporation of the solvent a solid was formed which was collected on a glass filter, yielding 4.3 g of a white solid. Back-extraction of the wash solution yielded another batch of 4.0 g of equally pure title compound (total amount of **12** obtained = 8.3 g, quantitative). $^1\text{H NMR}$, DMSO- d_6 (500 MHz), δ (ppm): 8.09 (s, 1H), 7.94 (d, $J = 2.1\text{ Hz}$, 1H), 7.55 (d, $J = 8.0\text{ Hz}$, 1H), 7.25 (dd, $J = 8.0\text{ Hz}$, $J = 2.1\text{ Hz}$, 1H), 5.14 (s, 2H), 1.57 (s, 9H). LCMS (method C): $M - \text{tBu} + \text{H}^+$ (t_R) = 254.2 (0.96 min).

5-Chloro-1-[2-(4-methylpiperazin-1-yl)-2-oxoethyl]-1H-indole-3-carboxylic Acid tert-Butyl Ester (13). To a solution of **12** (3.15 g, 10.0 mmol) in DMF (70 mL) were added EDC-HCl (2.93 g, 20.0 mmol) and pentafluorophenol (2.81 g, 15.0 mmol). After 20 min, *N*-ethylmorpholine (3.80 mL, 30.0 mmol) and 1-methylpiperazine (1.1 mL, 10.0 mmol) were added and the reaction mixture was stirred for 12 h at room temperature. After this time the reaction mixture was concentrated and taken up with DCM and washed twice with an aqueous LiCl solution (4% w/w). The organic layer was dried over MgSO_4 and the crude product obtained after evaporation was purified by chromatography on silica gel, eluting with a gradient of EtOAc/MeOH to afford **13** (2.26 g, 58%). $^1\text{H NMR}$, DMSO- d_6 (500 MHz), δ (ppm): 8.05 (s, 1H), 7.99 (d, $J = 2.1\text{ Hz}$, 1H), 7.48 (d, $J = 8.8\text{ Hz}$, 1H), 7.23 (dd, $J = 8.8\text{ Hz}$, $J = 2.1\text{ Hz}$, 1H), 5.34 (s, 2H), 3.58 (m, 2H), 3.47 (m, 2H), 2.44 (m, 2H), 2.31 (m, 2H), 2.24 (s, 3H), 1.58 (s, 9H). LCMS (method C): $M - \text{tBu} + \text{H}^+$ (t_R) = 336.2 (0.73 min).

5-Chloro-1-[2-(4-methylpiperazin-1-yl)-2-oxoethyl]-1H-indole-3-carboxylic Acid (4h'). To a solution of **13** (2.26 g, 5.80 mmol) in DCM (30 mL) was added TFA (4.3 mL, 56.1 mmol). After being stirred for 3 h, the reaction mixture was concentrated and co-distilled twice with toluene. The residue thus obtained was dissolved in MeCN/ H_2O and freeze-dried after addition of 7.3 mL of aqueous 2 N HCl. This procedure was repeated once to give **4h'** in its hydrochloride form (2.33 g, quantitative). $^1\text{H NMR}$, DMSO- d_6 (500 MHz), δ (ppm): 11.25 (br, 1H), 7.99 (s, 1H), 7.97 (d, $J = 2.1\text{ Hz}$, 1H), 7.54 (d, $J = 8.3\text{ Hz}$, 1H), 7.25 (dd, $J = 8.3\text{ Hz}$, $J = 2.1\text{ Hz}$, 1H), 5.45 (d, $J = 17.3\text{ Hz}$, 1H), 5.30 (d, $J = 17.3\text{ Hz}$, 1H), 4.37 (d, $J = 13.1\text{ Hz}$, 1H), 4.15 (d, $J = 13.1\text{ Hz}$, 1H), 3.62 (t, $J = 12.5\text{ Hz}$, 1H), 3.52 (d, $J = 12.1\text{ Hz}$, 1H), 3.43 (d, $J = 12.1\text{ Hz}$, 1H), 3.13 (m, 2H), 2.96 (m, 1H), 2.79 (s, 3H). LCMS (method C): MH^+ (t_R) = 336.2 (0.51 min).

1-[6-(4-Methoxybenzylamino)pyridazin-3-yl]-5-methyl-1H-pyrazole-4-carboxylic Acid Ethyl Ester (21). 4-Methoxybenzylamine (0.31 mL, 2.37 mmol) was added to a solution of ethyl 1-(6-chloropyridazin-3-yl)-5-methyl-1H-pyrazole-4-carboxylate (0.30 g, 1.13 mmol) in 1,4-dioxane (2 mL). Then it was heated at reflux for 2 h and evaporated to dryness. The residue was triturated with water, leading to the formation of a precipitate which was drained, dried under vacuum, taken up in isopropyl ether, drained again, and dried under vacuum to yield **21** (0.30 g, 72%). $^1\text{H NMR}$, DMSO- d_6 (250 MHz), δ (ppm): 8.03 (s, 1H), 7.67 (t, $J = 5.5\text{ Hz}$, 1H), 7.62 (d, $J = 9.2\text{ Hz}$, 1H), 7.32 (d, $J = 6.7\text{ Hz}$, 2H), 7.09 (d, $J = 9.2\text{ Hz}$, 1H), 6.91 (d, $J = 6.7\text{ Hz}$, 2H), 4.55 (d, $J = 5.5\text{ Hz}$, 2H), 4.26 (q, $J = 7.0\text{ Hz}$, 2H), 3.74 (s, 3H), 2.69 (s, 3H), 1.30 (t, $J = 7.0\text{ Hz}$, 3H).

1-[6-(4-Methoxybenzylamino)pyridazin-3-yl]-5-methyl-1H-pyrazole-4-carboxylic Acid (22). A solution of **21** (5 g, 13.6 mmol) in EtOH (50 mL) was added to a solution of KOH (3.82 g, 68.2 mmol) in water (50 mL). It was heated at $80\text{ }^{\circ}\text{C}$ for 2 h. It was then evaporated to dryness, and the residue was taken up in water (100 mL). An aqueous 1 N HCl of solution (68.0 mL, 68.0 mmol) was added dropwise under stirring and the precipitate that formed was drained, washed with water, and then dried in a vacuum stove to afford **22** as a white powder (4.5 g, 98%). $^1\text{H NMR}$, DMSO- d_6 (250 MHz), δ (ppm): 8.42 (br, 1H), 8.04 (s, 1H), 7.81 (d, $J = 9.5\text{ Hz}$, 1H), 7.37–7.30 (m, 3H), 6.93 (d, $J = 6.9\text{ Hz}$, 2H), 4.57 (s, 2H), 3.75 (s, 3H), 2.71 (s, 3H).

1-[6-[*tert*-Butoxycarbonyl-(4-methoxybenzyl)amino]pyridazin-3-yl]-5-methyl-1*H*-pyrazole-4-carboxylic Acid (16w). DMAP (0.17 g, 1.38 mmol), Et₃N (2.32 mL, 16.5 mmol), and di-*tert*-butyl dicarbonate (3.01 g, 13.8 mmol) were successively added to a solution of **22** (1.87 g, 5.51 mmol) in DMF (22 mL). Then it was stirred for 20 h at room temperature. A solution of potassium hydroxide (0.46 g, 8.27 mmol) in water (10 mL) was added, and it was stirred for 20 h. Water (500 mL) was added, and it was washed with ether. The aqueous phase was buffered with phosphate buffer preloaded with aqueous 1 N HCl. The precipitate that formed was drained, washed with water, and dried in a vacuum stove at 50 °C to afford **16w** (1.35 g, 56%). ¹H NMR, DMSO-*d*₆ (250 MHz), δ (ppm): 12.7 (br, 1H), 8.21–8.05 (m, 3H), 7.25 (d, *J* = 8.7 Hz, 1H), 6.88 (d, *J* = 8.7 Hz, 1H), 5.19 (br, 2H), 3.71 (s, 3H), 2.83 (s, 3H), 1.43 (s, 9H).

3-(1-[6-[*tert*-Butoxycarbonyl-(4-methoxybenzyl)amino]pyridazin-3-yl]-5-methyl-1*H*-pyrazol-4-yl]-3-oxopropionic Acid Ethyl Ester (17w). 1,1'-Carbonyldiimidazole (0.53 g, 3.25 mmol) was added to a solution of **16w** (1.1 g, 2.50 mmol) in THF (17 mL), and it was stirred for 20 h at room temperature. Magnesium bis(3-ethoxy-3-oxopropanoate) (0.82 g, 2.88 mmol) was added, and it was stirred at 55 °C for 20 h. EtOAc (50 mL) was added. It was washed with aqueous 0.1 N NaOH, with brine, dried over Na₂SO₄, and evaporated to dryness. It was purified by silica gel chromatography, eluting with DCM and then eluting with DCM/MeOH mixture (95/5; v/v) to afford **23w** in the form of a white powder (1.18 g, 92%). ¹H NMR, DMSO-*d*₆ (250 MHz), δ (ppm): 8.41 (s, 1H), 8.22 (d, *J* = 9.5 Hz, 1H), 8.09 (d, *J* = 9.5 Hz, 1H), 7.25 (d, *J* = 6.5 Hz, 2H), 6.88 (d, *J* = 6.5 Hz, 2H), 5.19 (s, 2H), 4.13 (q, *J* = 7.2 Hz, 2H), 4.04 (s, 2H), 3.72 (s, 3H), 2.82 (s, 3H), 1.43 (s, 9H), 1.21 (t, *J* = 7.2 Hz, 3H).

2-(1-[6-[*tert*-Butoxycarbonyl-(4-methoxybenzyl)amino]pyridazin-3-yl]-5-methyl-1*H*-pyrazole-4-carbonyl)butyric Acid Ethyl Ester (18w). Potassium carbonate (1.25 g, 9.03 mmol), tetrabutylammonium bromide (0.98 g, 3.03 mmol), and iodoethane (0.44 mL, 4.51 mmol) were added to a solution of **17w** (1.15 g, 2.26 mmol) in THF (23 mL). Then it was stirred at 55 °C for 20 h. After it returned to room temperature, EtOAc (150 mL) was added and it was washed with water, with brine, dried over Na₂SO₄, and evaporated to dryness. It was purified by silica gel chromatography, eluting with DCM/MeOH mixture (97/3; v/v) to afford **18w** in the form of a white powder (1.18 g, 97%). ¹H NMR, DMSO-*d*₆ (250 MHz), δ (ppm): 8.49 (s, 1H), 8.22 (d, *J* = 9.5 Hz, 1H), 8.09 (d, *J* = 9.5 Hz, 1H), 7.25 (d, *J* = 8.7 Hz, 2H), 6.88 (d, *J* = 8.7 Hz, 2H), 5.19 (s, 2H), 4.28 (t, *J* = 7.2 Hz, 1H), 4.10 (q, *J* = 7.2 Hz, 2H), 3.72 (s, 3H), 2.82 (s, 3H), 1.88 (quint, *J* = 7.2 Hz, 2H), 1.43 (s, 9H), 1.15 (t, *J* = 7.2 Hz, 3H), 0.92 (t, *J* = 7.2 Hz, 3H).

1-[1-(6-Aminopyridazin-3-yl)-5-methyl-1*H*-pyrazol-4-yl]-butan-1-one (20w). A solution of **18w** (1.18 g, 2.19 mmol) in aqueous 37% HCl (4.4 mL) was heated at 105 °C for 6 h. After it returned to room temperature, water was added (50 mL), and it was washed twice with EtOAc. Then the aqueous phase was evaporated to dryness. A 0.2 N solution (50 mL) was added to the solid residue, and it was extracted with EtOAc. The organic phase was washed with brine, dried over Na₂SO₄, and evaporated to dryness to afford **20w** as a white powder (0.42 g, 78%). ¹H NMR, DMSO-*d*₆ (250 MHz), δ (ppm): 8.27 (s, 1H), 7.59 (d, *J* = 9.4 Hz, 1H), 7.00 (d, *J* = 9.4 Hz, 1H), 6.76 (br, 2H), 2.82 (t, *J* = 7.2 Hz, 2H), 2.65 (s, 3H), 1.62 (sext, *J* = 7.2 Hz, 2H), 0.93 (t, *J* = 7.2 Hz, 3H).

5-Methyl-1-trityl-1*H*-pyrazole-4-carboxylic Acid (33). A solution of 5-methyl-1*H*-pyrazole-4-carboxylic acid methyl ester (6.60 g, 47.1 mmol), potassium carbonate (8.46 g, 61.22 mmol), and trityl chloride (15.8 g, 56.5 mmol) in DMF (50 mL) was stirred at room temperature during 5 days. EtOAc was added and the organic phase was washed with water, with brine, dried over Na₂SO₄, and evaporated to dryness. The oily residue was suspended in EtOH/H₂O (100 mL, 50/50 v/v). Then potassium hydroxide (9.95 g, 177 mmol) was added, and the reaction mixture was refluxed during 6 h. The hot mixture was drained, and the filtrate was reduced to remove EtOH. An aqueous 1 N HCl solution was added and the precipitate that formed was filtered, washed with a isopropyl ether/EtOAc mixture (50/50 v/v), and dried at 50 °C under vacuum to afford **33** as a white powder (9.70 g, 56%).

It should be noted that some more expected compound was present in the filtrate. ¹H NMR, DMSO-*d*₆ (250 MHz), δ (ppm): 7.61 (s, 1H), 7.43–7.34 (m, 9H), 7.09–7.03 (m, 6H), 2.33 (s, 3H).

5-Methyl-1-trityl-1*H*-pyrazole-4-carboxylic Acid Methoxymethylamide (34). To a solution of **33** (9.70 g, 26.3 mmol), DMAP (10.3 g, 84.3 mmol), and BOP-Cl (10.3 g, 39.5 mmol) in DCM (100 mL) was added *N,O*-dimethylhydroxylamine hydrochloride (3.856 g, 39.5 mmol). The reaction mixture was stirred at room temperature for 1 h and evaporated to dryness. The residue was dissolved in EtOAc, and the organic phase was washed with water, with brine, dried over Na₂SO₄, and evaporated to dryness. The solid residue was triturated with isopropyl ether, filtered, and dried under vacuum at 50 °C to afford **34** as a white powder (10.4 g, 87%). ¹H NMR, DMSO-*d*₆ (250 MHz), δ (ppm): 7.71 (s, 1H), 7.44–7.33 (m, 9H), 7.15–7.05 (m, 6H), 3.39 (s, 3H), 3.13 (s, 3H), 2.34 (s, 3H).

1-(5-Methyl-1-trityl-1*H*-pyrazol-4-yl)butan-1-one (35). To a solution of **34** (10.4 g, 25.2 mmol) in anhydrous THF (130 mL) at –30 °C was added drop by drop a 2 M *n*-propylmagnesium chloride solution in ether (32.7 mL, 65.4 mmol). The mixture was allowed to return to room temperature, and it was then stirred for 4 h. The reaction mixture was cooled to –30 °C, and water (50 mL) was added drop by drop. After the mixture returned to room temperature, an aqueous 1 N HCl solution (250 mL) was added and the aqueous phase was extracted with EtOAc (3×). The combined organic phases were washed with water, with brine, dried over Na₂SO₄, and evaporated to dryness. The solid residue was triturated with isopropyl ether, filtered, and dried under vacuum at 50 °C to afford **35** as a white powder (8.4 g, 85%). ¹H NMR, DMSO-*d*₆ (400 MHz), δ (ppm): 7.93 (s, 1H), 7.45–7.33 (m, 9H), 7.12–7.04 (m, 6H), 2.62 (t, *J* = 7.2 Hz, 2H), 2.34 (s, 3H), 1.52 (sext, *J* = 7.2 Hz, 2H), 0.84 (t, *J* = 7.2 Hz, 3H).

1-(5-Methyl-1*H*-pyrazol-4-yl)butan-1-one (36). **35** (8.4 g, 21.3 mmol) was stirred in a 4 N solution of HCl in 1,4-dioxane (50 mL) during 6 h. The reaction mixture was evaporated to dryness, and the solid residue was triturated with isopropyl ether, filtered, and dried under vacuum at 50 °C to afford **36** as a white powder (2.00 g, 62%). It should be noted that evaporation of the filtrate allowed isolation of a new batch with slightly less purity (1.10 g, 34%). ¹H NMR, DMSO-*d*₆ (250 MHz), δ (ppm): 8.15 (s, 1H), 2.71 (t, *J* = 7.0 Hz, 2H), 2.39 (s, 3H), 1.58 (sext, *J* = 7.0 Hz, 2H), 0.90 (t, *J* = 7.0 Hz, 3H).

3-(*tert*-Butyldimethylsilyloxy)pentanedioic Acid Dimethyl Ester (37). To a solution of TBDMSCl (28.2 g, 187 mmol) and imidazole (30.2 g, 443 mmol) in DCM (225 mL) was slowly added a solution of dimethyl 3-hydroxyglutarate (30 g, 170 mmol) in DCM (225 mL). After the mixture was stirred overnight water was added, the layers were separated, and the aqueous layer was extracted twice with DCM. The combined organic layers were dried over MgSO₄, and the crude product obtained after evaporation was purified by chromatography on silica gel, eluting with a gradient of EtOAc/*n*-heptane. The fractions containing the product were combined and the solvent was evaporated under reduced pressure to yield **37** (45.0 g, 91%). ¹H NMR, CDCl₃ (400 MHz), δ (ppm): 4.50 (quint, 1H), 3.62 (s, 6H), 2.50 (d, 6H), 0.80 (s, 9H), 0.00 (s, 6H).

3-(*tert*-Butyldimethylsilyloxy)pentane-1,5-diol (38). To a solution of **37** (13.5 g, 46.5 mmol) in ether (750 mL) was added successively lithium borohydride (6.00 g, 279 mmol) at 0 °C. After the mixture was stirred overnight saturated aqueous ammonium chloride was added and the mixture extracted twice with DCM. After evaporation of the solvent the crude product **38** was obtained (11.9 g, quantitative). ¹H NMR, DMSO-*d*₆ (400 MHz), δ (ppm): 4.28 (t, *J* = 5.4 Hz, 2H), 3.86 (quint, *J* = 6.0 Hz, 1H), 3.41 (m, 4H), 1.52 (m, 4H), 0.82 (s, 9H), 0.00 (s, 6H).

[4-(*tert*-Butyldimethylsilyloxy)piperidin-1-yl]carbamic Acid *tert*-Butyl Ester (39). To a solution of oxalyl chloride (13.3 mL, 152 mmol) in DCM (700 mL) was added dropwise a solution of DMSO (14.4 mL, 203 mmol) in 160 mL of DCM at –78 °C. After 30 min, a solution of **38** (11.9 g, 50.8 mmol) in DCM (160 mL) was added at this temperature, followed by the addition of Et₃N (70.7 mL, 508 mmol) after 30 min. After stirring for 1 h, it was warmed to 0 °C and stirred an additional 30 min at this temperature. It was diluted with toluene (92 mL), filtered via a glass frit, and the filtrate was

concentrated. After resuspension with pentane it was filtered via a plug of Celite to give the crude dialdehyde (13.5 g, quantitative) after evaporation of the solvent. To a solution of crude dialdehyde (12.0 g, ~52.1 mmol) and *tert*-butyl carbazate (7.60 g, 57.3 mmol) in DCM (350 mL) was added sodium triacetoxyborohydride (26.5 g, 125 mmol) at 0 °C. After the mixture was stirred overnight, saturated aqueous NaHCO₃ was added and the layers were separated. The aqueous layer was extracted twice with DCM to give the crude product after evaporation of the solvent. Purification was performed by chromatography on silica gel, eluting with a gradient of EtOAc/*n*-heptane. The fractions containing the product were combined and the solvent was evaporated under reduced pressure to afford **39** (8.6 g, 50%). ¹H NMR, DMSO-*d*₆ (400 MHz), δ (ppm): 7.86 (br, 1H), 3.64 (m, 1H), 2.77 (m, 2H), 2.52 (m, 2H), 1.65 (m, 2H), 1.43 (m, 2H), 1.33 (s, 9H), 0.83 (s, 9H), 0.00 (s, 6H).

(4-Hydroxypiperidin-1-yl)carbamic Acid *tert*-Butyl Ester (40). To a solution of **39** (8.60 g, 26.0 mmol) in THF (400 mL) was added 1 M TBAF in THF (28.6 mL, 28.6 mmol) at 0 °C. After the mixture was stirred for 12 h, additional 28.6 mL of TBAF solution was added and the reaction mixture stirred for 12 h. It was then concentrated, redissolved in DCM, and extracted three times with water. The combined aqueous layers were reextracted with DCM/*i*-PrOH 3:1, and the combined organic fractions were evaporated. Purification was performed by chromatography on silica gel, eluting with a gradient of EtOAc/*n*-heptane. The fractions containing the product were combined and the solvent was evaporated under reduced pressure, affording **40** (4.35 g, 78%). ¹H NMR, DMSO-*d*₆ (400 MHz), δ (ppm): 7.89 (br, 1H), 4.55 (d, *J* = 3.8 Hz, 1H), 3.43 (m, 1H), 2.78 (m, 2H), 2.52 (m, 2H), 1.67 (m, 2H), 1.48–1.36 (m, 11H).

Methanesulfonic Acid 1-*tert*-Butoxycarbonylaminopiperidin-4-yl Ester (41). To a solution of **40** (4.35 g, 19.7 mmol) in DCM (100 mL) were successively added DMAP (0.24 g, 2.00 mmol), Et₃N (2.80 mL, 20.6 mmol), and methanesulfonyl chloride (1.50 mL, 19.7 mmol). After the mixture was stirred overnight, it was diluted with DCM and washed twice with aqueous 0.1 M HCl. The aqueous layer was reextracted with DCM, and the combined organic fractions yielded the crude product **41** as colorless oil (6.0 g, quantitative). ¹H NMR, DMSO-*d*₆ (500 MHz), δ (ppm): 8.39 (br, 1H), 4.76 (m, 1H), 3.24 (s, 3H), 2.92 (m, 2H), 2.78 (m, 2H), 1.95 (m, 2H), 1.83 (m, 2H), 1.40 (s, 9H).

[4-(4-Butyryl-5-methylpyrazol-1-yl)piperidin-1-yl]carbamic Acid *tert*-Butyl Ester (42). To a solution of **36** (1.55 g, 10.2 mmol) in DMF (15 mL) was added potassium *tert*-butoxide (1.20 g, 10.7 mmol), and the solution was stirred at 50 °C for 30 min. Then a solution of **41** (3.00 g, 10.2 mmol) in DMF (5 mL) was added and further stirred at this temperature. Additional potassium *tert*-butoxide (3 × 300 mg after 12 h each) was added in order to increase the conversion. It was concentrated, diluted with DCM, and washed with water three times. The crude product thus obtained was purified by preparative HPLC (C18 reverse phase column, elution with a H₂O/MeCN gradient with 0.1% TFA). The fractions containing the product were evaporated and lyophilized to yield 0.96 g of a mixture of the title compound and its position isomer. Further HPLC purification on chiral stationary phase yielded the desired *N*-alkylated pyrazole **42** (0.36 g, 10%). ¹H NMR, DMSO-*d*₆ (500 MHz), δ (ppm): 8.49 (br, 1H), 8.03 (s, 1H), 4.22 (m, 1H), 3.05 (d, *J* = 10.4 Hz, 2H), 2.81 (t, *J* = 10.4 Hz, 2H), 2.73 (t, *J* = 7.2 Hz, 2H), 2.54 (s, 3H), 2.13 (m, 2H), 1.82 (m, 2H), 1.57 (sext, *J* = 7.2 Hz, 2H), 1.39 (s, 9H), 0.90 (t, *J* = 7.2 Hz, 3H).

Hydrochloride Salt of 1-[1-(1-Aminopiperidin-4-yl)-5-methyl-1*H*-pyrazol-4-yl]butan-1-one (20ae). To a solution of **42** (0.54 g, 1.53 mmol) in DCM (12 mL) was added TFA (3.30 mL, 45.9 mmol). After stirring for 3 h at room temperature, the reaction mixture was concentrated and co-distilled twice with toluene. The residue thus obtained was dissolved in MeCN/H₂O and freeze-dried after addition of aqueous 2 N HCl (2.0 mL). This procedure was repeated once to give the crude hydrochloride salt of **20ae** (0.35 g, 74%). ¹H NMR, DMSO-*d*₆ (500 MHz), δ (ppm): 8.10 (s, 1H), 4.43 (m, 1H), 3.36 (m, 2H), 2.90 (br, 2H), 2.71 (t, *J* = 7.2 Hz, 2H), 2.55 (s, 3H), 2.15 (m,

2H), 1.96 (d, *J* = 12.2 Hz, 2H), 1.57 (sext, *J* = 7.2 Hz, 2H), 0.89 (t, *J* = 7.2 Hz, 3H).

{3-[6-(4-Butyryl-5-methylpyrazol-1-yl)pyridazin-3-ylcarbomoyl]-5-chloroindol-1-yl}acetic Acid Methyl Ester (46w). To a solution of **4h** (6.00 g, 22.4 mmol) in DCM (200 mL) were added DMF (few drops) and thionyl chloride (6.60 mL, 89.7 mmol). After 3 h under reflux, the reaction mixture was evaporated to dryness and the solid residue was triturated with DCM (80 mL), filtered, and washed with DCM, thus producing (5-chloro-3-chlorocarbonylindol-1-yl)-acetic acid methyl ester as a white powder (4.5 g).

A solution of **20w** (0.35 g, 1.43 mmol) and DMAP (0.59 g, 4.84 mmol) was stirred for 30 min in the presence of 4 Å molecular sieves (1.00 g) in 1,2-dichloroethane (20 mL). (5-Chloro-3-chlorocarbonylindol-1-yl)acetic acid methyl ester (0.92 g, 3.21 mmol) was added, and the reaction mixture was stirred at 80 °C for 6 h. After the mixture returned to room temperature, the molecular sieves were removed by filtration. The filtrate was washed with water, with brine, dried over Na₂SO₄, and evaporated under vacuum. The solid residue was purified by silica gel chromatography, eluting with DCM/MeOH mixture (gradient from 0% to 5% of MeOH), obtaining **46w** as a white powder (0.51 g, 72% from **20w**). ¹H NMR, DMSO-*d*₆ (250 MHz), δ (ppm): 11.42 (br, 1H), 8.71 (d, *J* = 9.5 Hz, 1H), 8.65 (s, 1H), 8.41 (s, 1H), 8.23 (s, 1H), 8.13 (d, *J* = 9.5 Hz, 1H), 7.62 (d, *J* = 8.7 Hz, 1H), 7.32 (d, *J* = 8.7 Hz, 1H), 5.33 (s, 2H), 3.73 (s, 3H), 2.87 (t, *J* = 7.2 Hz, 2H), 2.82 (s, 3H), 1.64 (sext, *J* = 7.2 Hz, 2H), 0.94 (t, *J* = 7.2 Hz, 3H).

{3-[4-(4-Butyryl-5-methylpyrazol-1-yl)phenylcarbomoyl]-5-methylindol-1-yl}acetic Acid (50a). To **46a** (10.0 g, 21.1 mmol) in MeOH (100 mL) was added aqueous 2 N NaOH (15.9 mL, 31.7 mmol). It was stirred at room temperature overnight and then concentrated under vacuum. The residue was suspended in aqueous 1 N HCl, then filtered, washed with water, and dried under vacuum to afford **50a** as a white powder (9.47 g, 98%). ¹H NMR, DMSO-*d*₆ (250 MHz), δ (ppm): 13.19 (br, 1H), 10.02 (s, 1H), 8.24 (s, 1H), 8.23 (s, 1H), 8.02 (s, 1H), 7.95 (d, *J* = 9.0 Hz, 2H), 7.49 (d, *J* = 9.0 Hz, 2H), 7.39 (d, *J* = 8.5 Hz, 1H), 7.08 (d, *J* = 8.5 Hz, 1H), 5.13 (s, 2H), 2.82 (t, *J* = 7.2 Hz, 2H), 2.50 (s, 3H), 2.43 (s, 3H), 1.64 (sext, *J* = 7.2 Hz, 2H), 0.94 (t, *J* = 7.2 Hz, 3H). LCMS (method A): MH⁺ (*t*_R) = 459 (8.31 min). Mp = 201 °C.

{3-[6-(4-Butyryl-5-methylpyrazol-1-yl)pyridazin-3-ylcarbomoyl]-5-chloroindol-1-yl}acetic Acid (50w). Same procedure was used as for **50a** in dioxane (2.07 g, 69%). ¹H NMR, DMSO-*d*₆ (400 MHz), δ (ppm): 13.25 (br, 1H), 11.35 (s, 1H), 8.68 (d, *J* = 8.0 Hz, 1H), 8.66 (s, 1H), 8.40 (s, 1H), 8.23 (s, 1H), 8.13 (d, *J* = 8.0 Hz, 1H), 7.61 (d, *J* = 8.8 Hz, 1H), 7.30 (d, *J* = 8.8 Hz, 1H), 5.17 (s, 2H), 2.86 (t, *J* = 7.2 Hz, 2H), 2.82 (s, 3H), 1.65 (sext, *J* = 7.2 Hz, 2H), 0.93 (t, *J* = 7.2 Hz, 3H).

Hydrochloride Salt of *N*-[6-(4-Butanoyl-5-methyl-1*H*-pyrazol-1-yl)pyridazin-3-yl]-5-chloro-1-[2-(4-methylpiperazin-1-yl)-2-oxoethyl]-1*H*-indole-3-carboxamide (52w). 1-Methylpiperazine (1.66 g, 16.5 mmol), pyridine (2.23 mL, 27.6 mmol), and BOP-Cl (4.30 g, 16.5 mmol) were added successively to **50w** (2.65 g, 5.51 mmol) in solution in DMF (80 mL). The reaction mixture was stirred for 48 h. Then it was poured into a biphasic mixture of EtOAc and saturated aqueous NaHCO₃. The precipitate formed was filtered and washed with isopropyl ether. The filtrate was transferred to a separating funnel, and the organic phase was washed with water, with brine and then dried over Na₂SO₄. The organic phase was concentrated partially, and the precipitate formed was filtered. The two precipitates were combined and dried in a vacuum stove. It was suspended in MeOH (200 mL). Then a 1 N HCl solution in ether (6.60 mL, 6.60 mmol) was added, and it was stirred for 1 h. The precipitate that formed was drained. It was washed with isopropyl ether and then dried in a vacuum stove at 40 °C, obtaining **52w** (2.29 g, 69%) as a light yellow powder. ¹H NMR, DMSO-*d*₆ (400 MHz), δ (ppm): 11.38 (s, 1H), 10.97 (br, 1H), 8.71 (d, *J* = 9.6 Hz, 1H), 8.58 (s, 1H), 8.41 (s, 1H), 8.24 (s, 1H), 8.14 (d, *J* = 9.6 Hz, 1H), 7.59 (d, *J* = 8.8 Hz, 1H), 7.30 (d, *J* = 8.8 Hz, 1H), 5.50 (d, *J* = 16 Hz, 1H), 5.35 (d, *J* = 16 Hz, 1H), 4.39–3.41 (m, 5H), 3.25–2.93 (m, 3H), 2.89–2.80 (m, 8H), 1.65 (sext, *J* = 7.2 Hz, 2H), 0.95 (t, *J* = 7.2 Hz, 3H). LCMS (method A): MH⁺ (*t*_R) = 563 (6.59 min). C 55.59%, H 5.35%,

N 18.46%, C₂₈H₃₁ClN₈O₃·HCl·0.1H₂O. Mp = 287 °C (crystal powder). Experimental log *D* = 2.71. Experimental p*K*_a = 6.3.

Hydrochloride Salt of *N*-[4-(4-Butanoyl-5-methyl-1*H*-pyrazol-1-yl)piperidin-1-yl]-5-chloro-1-[2-(4-methylpiperazin-1-yl)-2-oxoethyl]-1*H*-indole-3-carboxamide (52ae). To a solution of 4h' (0.337 g, 1.00 mmol) in DMF (45 mL) were added HOBt (0.152 g, 1.10 mmol), diisopropylethylamine (0.60 mL, 3.50 mmol), and EDC·HCl (0.191 g, 1.00 mmol). After 10 min, 20ae (0.330 g, 1.10 mmol) was added and the reaction mixture was stirred at room temperature during 24 h. EDC·HCl (0.095 g), HOBt (0.075 g), and diisopropylethylamine (0.30 mL) were added. After 24 h, the reaction was complete. The reaction mixture was evaporated under vacuum, and the residue was purified by preparative HPLC (reverse phase C18 column using a H₂O/acetonitrile gradient in the presence of TFA (0.1%). The solid residue was dissolved in a H₂O/acetonitrile mixture (1/1; v/v). Aqueous 1 N HCl (0.43 mL, 0.43 mmol) was added, and it was lyophilized. This procedure was repeated once to afford 52ae (0.186 g, 33%). ¹H NMR, DMSO-*d*₆ (500 MHz), δ (ppm): 11.30 (br, 1H), 8.22 (s, 1H), 8.11 (s, 1H), 8.09 (s, 1H), 7.57 (d, *J* = 9.0 Hz, 1H), 7.27 (d, *J* = 9.0 Hz, 1H), 5.48 (AB system, *J* = 17.0 Hz, 1H), 5.34 (AB system, *J* = 17.0 Hz, 1H), 4.57 (br, 1H), 4.35 (d, *J* = 13.6 Hz, 2H), 4.17 (d, *J* = 13.6 Hz, 2H), 3.70–3.39 (m, 6H), 3.16 (m, 2H), 2.98 (m, 1H), 2.81 (d, *J* = 4.6 Hz, 3H), 2.75 (t, *J* = 7.2 Hz, 2H), 2.59 (s, 3H), 2.42 (m, 2H), 2.05 (m, 2H), 1.57 (sext, *J* = 7.2 Hz, 2H), 0.90 (t, *J* = 7.2 Hz, 3H).

Binding Experiments. [³³P]2-MeS-ADP binding was measured on P2Y₁₂-expressing CHO cells using a previously reported filtration technique to separate the free from bound [³³P]2-MeSADP.³⁰ Incubations were performed in a total of 200 μL of binding buffer (phosphate buffered saline [PBS], 1 mM EDTA 0.2%, w/v bovine serum albumin) containing CHO cells (35 × 10³/sample) and [³³P]2-MeS-ADP (0.16 nM, 0.15 × 10⁶ dpm/sample). The tested compounds were incubated for 30 min with cells. Triplicate incubations with radioactive ligand were carried out at 20 °C for 15 min and were terminated by the addition of 3 mL of ice-cold assay buffer followed by rapid vacuum filtration over glass-fiber filters (Filtermats 11734, Skatron Instruments Inc., Sterling, VA, USA). Filters were then washed twice with 5 mL of ice-cold PBS, dried, and the radioactivity was measured by scintillation counting. Nonspecific binding was defined as the total binding measured in the presence of excess unlabeled ADP (1 mM), and specific binding was defined as the difference between total binding and nonspecific binding. The percent inhibition was expressed as %I = [(total binding – total binding with antagonist)/specific binding] × 100. The IC₅₀ value was defined as the concentration of inhibitor required to obtain 50% inhibition of the specific binding. Concentration–response curves were analyzed with internal software using the four-parameter logistic modeling according to the method of Ratkowsky and Reedy.³¹ The adjustment was obtained by nonlinear regression using the Marquardt algorithm in SASR software (version 9.1 UNIX, SAS Institute, Cary, NC, USA). Parameter estimations were obtained using % inhibition with lower asymptotes and upper asymptotes constrained at 0 and 100, respectively.

Inhibition of Platelet Aggregation in Vitro (Human Blood). The blood is taken from healthy volunteers, using 20 mL syringes containing 2 mL of buffered sodium citrate. The blood is transferred to polypropylene tubes and centrifuged for 5 min (100g) at room temperature (without using the brake of the centrifuge). The supernatant platelet-rich plasma (PRP) is then removed, diluted, and the platelets are counted before they are used in aggregation measurements.

The measurements of platelet aggregation are performed at 37 °C in glass tubes (Chrono-Log Kordia aggregometer). An amount of 4 μL of the test compound (solution 100 times more concentrated than the required final concentration, in DMSO) is mixed with 392 μL of fresh PRP, and the mixture was incubated for 1 min with stirring. Then 4 μL of a solution of ADP at 250 μM is added to the mixture. The measurements of aggregation are monitored for 6–8 min, stirring continuously, by recording the variations of optical density according to the method of G. V. Born.³² The results are calculated using the

aggregation amplitude expressed as height and are expressed as percentage inhibition. The compounds have CI₅₀ (of inhibition of platelet aggregation) between 0.1 and 2 μM.

Inhibition of Platelet Aggregation in Vitro (Rat Blood). The blood is taken from male rats of the Sprague–Dawley strain, weighing 250–300 g. The sample is taken on sodium citrate at 3.8% (1 volume to 9 volumes of blood) by puncture of the abdominal aorta after anesthetizing the animal with pentobarbital sodium. The platelet-rich plasma (PRP) is obtained by centrifugation of the blood at 300g for 5 min, and the measurements of platelet aggregation are performed as described above. The results are calculated using the area under the curve of absorbance measured for 6 min and expressed as percentage inhibition. The compounds have CI₅₀ values (of inhibition of platelet aggregation) between 0.02 and 1.5 μM.

Inhibition of Platelet Aggregation ex Vivo (Rat Blood). Male rats of the Sprague–Dawley strain, weighing 250–300 g, are used at a rate of 6 animals per batch. Each test compound is diluted in a solution of glucose-containing water (glucose 5%) containing 5% of Cremophor and 3% of glycofurol and administered by stomach tube (10 mL/kg at 1 mg/mL) 2 h before taking the sample. The sample is taken on sodium citrate at 3.8% (1 volume to 9 volumes of blood) by puncture of the abdominal aorta after anesthetizing the animal with pentobarbital sodium.

The platelet-rich plasma (PRP) is obtained by centrifugation of the blood at 300g for 5 min, and the measurements of platelet aggregation are performed as described above. The results are calculated using the area under the curve of absorbance measured for 6 min and expressed as percentage (%) of inhibition.

■ ASSOCIATED CONTENT

📄 Supporting Information

Selectivity data for SAR216471, analytical data (¹H NMR) and synthetic methods for reaction intermediates, analytical data (¹H NMR, LCMS, elemental analysis, melting points) and synthetic methods for final compounds. This material is available free of charge via the Internet at <http://pubs.acs.org>.

■ AUTHOR INFORMATION

Corresponding Author

*E-mail: christophe.boldron@sanofi.com. Phone: +33534633089.

Notes

The authors declare no competing financial interest.

■ ACKNOWLEDGMENTS

The authors thank Dr. J.-P. Maffrand for constant support and strong scientific challenge, Dr. A. Lindenschmidt, Dr. V. Wehner, and Dr. H. Heitsch (Sanofi R&D, Frankfurt, Germany) for scientific challenge, Dr. P. Hamley and colleagues (Sanofi R&D, Frankfurt, Germany) for library synthesis, Dr. C. Ponthus, Dr. E. Cogo, Dr. J. Menegotto, and colleagues (Sanofi R&D, Toulouse, France) for their essential support in structural determinations, early formulation, and solid state studies, Dr. S. Maignan and Dr. J. P. Rameau (Sanofi R&D, Toulouse, France) for in silico chemistry support, J. C. Bourbier, G. Basquin, and G. Manette (Sanofi R&D, Chilly-Mazarin, France) for synthetic chemistry support. Also, special thanks are given to L. Laplanche, F. Sadoun, E. Erdociain, P. Cardon, P. Dupont, G. Fabre, and colleagues from the DSAR Department (Sanofi R&D, Montpellier, France) for their support in ADME studies and to A. R. Jost and K. Braun (Sanofi R&D, Frankfurt, Germany) for the Ames II *Salmonella* evaluations.

■ ABBREVIATIONS USED

AA, antiaggregant activity; aq, aqueous; Bnd, binding; BOP-Cl, bis(2-oxo-3-oxazolidinyl)phosphinic chloride; Caco-2, colon adenocarcinoma; CHO, Chinese hamster ovary; CRE-Luc, luciferase-directed cAMP response elements; EDC·HCl, N-(3-dimethylaminopropyl)-N'-ethylcarbodiimide hydrochloride; EF, eligibility factor; HOBt, 1-hydroxybenzotriazole; MPK, metabolism and pharmacokinetics; POC, proof of concept; PRP, platelet rich plasma; TBDMSCl, *tert*-butyldimethylsilyl chloride

■ REFERENCES

(1) Kunapuli, S. P. P2 receptors and platelet activation. *TheScientificWorldJournal* **2002**, *2*, 424–433.

(2) Kauffenstein, G.; Bergmeier, W.; Eckly, A.; Ohlmann, P.; Leon, C.; Cazenave, J. P.; Nieswandt, B.; Gachet, C. The P2Y12 receptor induces platelet aggregation through weak activation of the $\alpha IIb\beta 3$ integrin—a phosphoinositide 3-kinase-dependent mechanism. *FEBS Lett.* **2001**, *505* (2), 281–290.

(3) Maffrand, J. P. The story of clopidogrel and its predecessor, ticlopidine: Could these major antiplatelet and antithrombotic drugs be discovered and developed today? *C. R. Chim.* **2012**, *15*, 737–743.

(4) Angiolillo, D. J. The evolution of antiplatelet therapy in the treatment of acute coronary syndromes: from aspirin to the present day. *Drugs* **2012**, *72* (16), 2087–2116.

(5) Feliste, R.; Delebasse, D.; Simon, M. F.; Chap, H.; Defreyne, G.; Vallee, E.; Douste-Blazy, L.; Maffrand, J. P. Effect of PCR 4099 on ADP-induced calcium movements and phosphatidic acid production in rat platelets. *Thromb. Res.* **1987**, *48* (4), 403–415.

(6) Holloper, G.; Jantzen, H. M.; Vincent, D.; Li, G.; England, L.; Ramakrishnan, V.; Yang, R. B.; Nurden, P.; Nurden, A.; Julius, D.; Conley, P. B. Identification of the platelet ADP receptor targeted by antithrombotic drugs. *Nature* **2001**, *409*, 202–207.

(7) Robert, A. N. Identification of the P2Y12 receptor: a novel member of the P2Y family of receptors activated by extracellular nucleotides. *Mol. Pharmacol.* **2001**, *60* (3), 416–420.

(8) (a) Savi, P.; Herbert, J. M. clopidogrel and ticlopidine: P2Y12 adenosine diphosphate-receptor antagonists for the prevention of atherothrombosis. *Semin. Thromb. Hemostasis* **2005**, *31*, 174–83. (b) CAPRIE Steering Committee. A randomised, blinded, trial of clopidogrel versus aspirin in patients at risk of ischaemic events (CAPRIE). *Lancet* **1996**, *348*, 1329–1339. (c) The Clopidogrel in Unstable Angina To Prevent Recurrent Events Trial Investigators. Effects of clopidogrel in addition to aspirin in patients with acute coronary syndromes without ST-segment elevation. *N. Engl. J. Med.* **2001**, *345*, 494–502.

(9) Niitsu, Y.; Jakubowski, J. A.; Sugidachi, A.; Asai, F. Pharmacology of CS-747 (prasugrel, LY640315), a novel, potent antiplatelet agent with in vivo P2Y12 receptor antagonist activity. *Semin. Thromb. Hemostasis* **2005**, *31*, 184–194.

(10) Savi, P.; Herbert, J. M.; Pflieger, A. M.; Dol, F.; Delebasse, D.; Combalbert, J.; Defreyne, G.; Maffrand, J. P. Importance of hepatic metabolism in the antiaggregating activity of the thienopyridine clopidogrel. *Biochem. Pharmacol.* **1992**, *44* (3), 527–532.

(11) Schroer, K. The basic pharmacology of ticlopidine and clopidogrel. *Platelets* **1993**, *4* (5), 252–261.

(12) (a) van Giezen, J. J.; Humphries, R. G. Preclinical and clinical studies with selective reversible direct P2Y12 antagonists. *Semin. Thromb. Hemostasis* **2005**, *31*, 195–204. (b) Springthorpe, B.; Bailey, A.; Barton, P.; Birkinshaw, T. N.; Bonnert, R. V.; Brown, R. C.; Chapman, D.; Dixon, J.; Guile, S. D.; Humphries, R. G.; Hunt, S. F.; Ince, F.; Ingall, A. H.; Kirk, I. P.; Leeson, P. D.; Leff, P.; Lewis, R. J.; Martin, B. P.; McGinnity, D. F.; Mortimore, M. P.; Paine, S. W.; Pairaudeau, G.; Patel, A.; Rigby, A. J.; Riley, R. J.; Teobald, B. J.; Tomlinson, W.; Webborn, P. J. H.; Willis, P. A. From ATP to AZD6140: the discovery of an orally active reversible P2Y12 receptor antagonist for the prevention of thrombosis. *Bioorg. Med. Chem. Lett.*

2007, *17*, 6013–6018. (c) Huber, K.; Hamad, B.; Kirkpatrick, P. Fresh from the pipeline. Ticagrelor. *Nat. Rev. Drug Discovery* **2011**, *10*, 255–256. (d) Gurbel, P. A.; Kereiakes, D. J.; Tantry, U. S. Ticagrelor for the treatment of arterial thrombosis. *Expert Opin. Pharmacother.* **2010**, *11*, 2251–2259.

(13) (a) Gurbel, P. A.; Kereiakes, D.; Tantry, U. S. Elinogrel Potassium. *Drugs Future* **2010**, *35*, 885–892. (b) Ueno, M.; Rao, S. V.; Angiolillo, D. J. Elinogrel: pharmacological principles, preclinical and early phase clinical testing. *Future Cardiol.* **2010**, *6*, 445–453. (c) Oestreich, J. H. Elinogrel, a reversible P2Y12 receptor antagonist for the treatment of acute coronary syndrome and prevention of secondary thrombotic events. *Curr. Opin. Invest. Drugs* **2010**, *11*, 340–348. (d) Berger, J. S.; Roe, M. T.; Gibson, C. M.; Kilaru, R.; Green, C. L.; Melton, L.; Blankenship, J. D.; Metzger, D. C.; Granger, C. B.; Gretler, D. D.; Grines, C. L.; Huber, K.; Zeymer, U.; Buszman, P.; Harrington, R. A.; Armstrong, P. W. Safety and feasibility of adjunctive antiplatelet therapy with intravenous elinogrel, a direct-acting and reversible P2Y12 ADP-receptor antagonist, before primary percutaneous intervention in patients with ST-elevation myocardial infarction: the early rapid reversal of platelet thrombosis with intravenous elinogrel before PCI to optimize reperfusion in acute myocardial infarction (ERASE MI). *Am. Heart J.* **2009**, *158*, 998–1004.

(14) Etter, M. C.; Urbakzyk-Lipkowska, Z.; Zia-Ebrahimi, S. M.; Panunto, T. W. Hydrogen bond directed cocrystallization and molecular recognition properties of diarylureas. *J. Am. Chem. Soc.* **1990**, *112*, 8415–8426.

(15) Dennis, M. S.; Zhang, M.; Meng, Y. G.; Kadkhodayan, M.; Kirchofer, D.; Combs, D.; Damico, L. A. Albumin binding as a general strategy for improving the pharmacokinetics of proteins. *J. Biol. Chem.* **2002**, *38*, 35035–35043.

(16) Ames, B. N.; Mccann, J.; Yamasaki, E. Methods for detecting carcinogens and mutagens with the *Salmonella*/mammalian-microsome mutagenicity test. *Mutat. Res.* **1975**, *31*, 347–364.

(17) Mortelmans, K.; Zeiger, E. The Ames *Salmonella*/microsome mutagenicity assay. *Mutat. Res.* **2000**, *455*, 29–60.

(18) (a) Helmick, J. S.; Martin, K. A.; Heinrich, J. L.; Novak, M. Mechanism of the reaction at carbon and nitrogen nucleophiles with the model carcinogens O-pivaloyl-N-arylhydroxylamines: competing SN2 substitution and SN1 solvolysis. *J. Am. Chem. Soc.* **1991**, *113*, 3459–3466. (b) Borosky, G. L. Ultimate carcinogenic metabolites from aromatic and heterocyclic aromatic amines: a computational study in relation to their mutagenic potency. *Chem. Res. Toxicol.* **2007**, *20*, 171–180.

(19) Dipple, A. DNA adducts of chemical carcinogens. *Carcinogenesis* **1995**, *16*, 437–441.

(20) (a) Benigni, R. Structure–activity relationship studies of chemical mutagens and carcinogens: mechanistic investigations and prediction approaches. *Chem. Rev.* **2005**, *105*, 1767–1800. (b) Benigni, R.; Giuliani, A.; Franke, R.; Gruska, A. Quantitative structure–activity relationship of mutagenic and carcinogenic aromatic amines. *Chem. Rev.* **2000**, *100*, 3697–3714. (c) Kadlubar, F. F.; Beland, F. A. Chemical Properties of Ultimate Carcinogenic Metabolites of Arylamines and Arylamides. *Polycyclic Hydrocarbons and Carcinogenesis*; American Chemical Society: Washington, DC, 1985; pp 341–370. (d) Chung, K. T.; Kirkovsky, L.; Kirkovsky, A.; Purcell, W. P. Review of Mutagenicity of Monocyclic Aromatic amines: quantitative structure–activity relationships. *Mutat. Res.* **1997**, *387*, 1–16. (e) Colvin, M. E.; Hatch, F. T.; Felton, J. S. Chemical and biological factors affecting mutagen potency. *Mutat. Res.* **1998**, *400*, 479–492. (f) Benigni, R.; Bossa, C.; Netzeva, T.; Rodomonte, A.; Tsakovska, I. Mechanistic QSAR of aromatic amines: new models for discriminating between homocyclic mutagens and nonmutagens, and validation of models for carcinogens. *Environ. Mol. Mutagen.* **2007**, *48*, 754–771. (g) Benigni, R.; Passerini, L. *Mutat. Res.* **2002**, *511*, 191–206.

(21) Kimball, R. F. The mutagenicity of hydrazine and some of its derivatives. *Mutat. Res.* **1977**, *39* (2), 111–126.

(22) Delesque-Touchard, N.; Pflieger, A. M.; Bonnet-Lignon, S.; Millet, L.; Salel, V.; Boldron, C.; Lassalle, G.; Herbert, J. M.; Savi, P.; Bono, F. SAR216471, an alternative to the use of currently available

P2Y₁₂ receptor inhibitors? *Thromb. Res.* [Online early access]. DOI: 10.1016/j.thromres.2014.06.034. Published Online: July 11, 2014.

(23) Mackie, R. K.; Mhatre, S.; Tedder, J. M. Carbon-trifluoroacylation—a convenient route to carboxylic acids. *J. Fluorine Chem.* **1977**, *10* (6), 437–445.

(24) Sakamoto, T.; Nagano, T.; Kondo, Y.; Yamanaka, H. Condensed heteroaromatic ring systems. XVII. Palladium-catalyzed cyclization of β -(2-halophenyl)amino substituted α,β -unsaturated ketones and esters to 2,3-disubstituted indoles. *Synthesis* **1990**, *3*, 215–218.

(25) Hwu, J. R.; Patel, H. V.; Lin, R. J.; Gray, M. O. Novel methods for the synthesis of functionalized indoles from arylhydroxylamines and activated acetylenes. *J. Org. Chem.* **1994**, *59*, 1577–1582.

(26) Duflosa, M.; Nourrissona, M. R.; Breleta, J.; Couranta, J.; LeBauta, G.; Grimaudb, N.; PetitbDuflos, J. Y. *N*-Pyridinylindole-3-(alkyl)carboxamides and derivatives as potential systemic and topical inflammation inhibitors. *Eur. J. Med. Chem.* **2001**, *36* (6), 545–553.

(27) Brooks, D. W.; Lu, L. D. L.; Masuniune, S. C-Acylation under virtually neutral conditions. *Angew. Chem., Int. Ed. Engl.* **1979**, *18*, 72–74.

(28) Hu, F. Z.; Zhang, G. F.; Liu, B.; Zou, X. M.; Zhu, Y. Q.; Yang, H. Z. A new method for the synthesis and herbicidal activity of 3-phenoxy-6-(1*H*-(substituted)pyrazol-1-yl) pyridazines. *J. Heterocycl. Chem.* **2009**, *46*, 584–590.

(29) Arvela, K.; Leadbeater, N. E. Fast and easy halide exchange in aryl halides. *Synlett* **2003**, *8*, 1145–1148.

(30) Savi, P.; Herbert, J. M. Use of radiolabeled 2-methylthio-ADP to study P2Y receptors on platelets and cell lines. *Methods Mol. Biol.* **2004**, *273*, 115–124.

(31) Ratkowsky, D. A.; Reedy, T. J. Choosing near-linear parameters in the four-parameter log model for radioligand and related assays. *Biometrics* **1986**, *42*, 575–582.

(32) Born, G. V. Aggregation of blood platelets by adenosine diphosphate and its reversal. *Nature* **1962**, *194*, 927–929.